Chaos, Solitons and Fractals 164 (2022) 112709

Contents lists available at ScienceDirect

Chaos, Solitons and Fractals

journal homepage: www.elsevier.com/locate/chaos

Modeling secondary infections with temporary immunity and disease enhancement factor: Mechanisms for complex dynamics in simple epidemiological models

Vanessa Steindorf [a,*,1], Akhil Kumar Srivastav [a,1], Nico Stollenwerk [a,1], Bob W. Kooi [b,1], Maíra Aguiar [a,c,d,*,1]

[a] Basque Center for Applied Mathematics - BCAM, Mazzaredo 14, Bilbao, 48009, Spain
[b] VU Amsterdam, Faculty of Science, De Boelelaan, 1085, Amsterdam, NL1081, The Netherlands
[c] Ikerbasque, Basque Foundation for Science, Euskadi Plaza, 5, Bilbao, 48009, Bizkaia, Spain
[d] Dipartimento di Matematica, Universita degli Studi di Trento, Via Sommarive, 14, Trento, 38123, Italy

ARTICLE INFO

Keywords:
Bifurcation analysis
Bi-stability
Chaos
Temporary immunity
Disease enhancement
Secondary infection

ABSTRACT

Modeling insights for epidemiological scenarios characterized by chaotic dynamics have been largely unexplored. A rigorous analysis of such systems are essential for a real predictive power and a more accurate disease control decision making. Motivated by dengue fever epidemiology, we study a basic SIR–SIR type model for the host population, capturing differences between primary and secondary infections. This model is the minimalistic version to previously suggested multi-strain models for dengue fever in which deterministic chaos was found in wider parameter regions. Without strain structure of pathogens, we consider temporary immunity after a primary infection and disease enhancement in a subsequent infection to identify to which extent these biological mechanisms can generate complex behavior in simple epidemiological models.

Stability analysis of the system is performed using the classical linearization theory, and the qualitative behavior of the model is investigated with a detailed bifurcation analysis. Rich dynamical structures are identified, including the Bogdanov–Takens, cusp and Bautin bifurcations which has never been described in dengue fever epidemiology. Besides the conventional transcritical bifurcation, a backward bifurcation occurs for higher disease enhancement in secondary infections, exhibiting bi-stability when biological temporary immunity period is assumed. The backward bifurcation is formalized using the center manifold theory. While the Hopf and the global homoclinic bifurcation curves were computed numerically, analytical expressions for the transcritical and tangent bifurcations are obtained. The combination of temporary immunity and disease enhancement play a significant role in the complexity of the system dynamics, with chaotic behavior observed after including seasonal forcing.

1. Introduction

Mathematical modeling has a long history in epidemiological research. Used as a tool to understand and predict disease transmission and control under different conditions, models incorporate different aspects of hosts, pathogen and environmental factors, which can imply rich dynamic behavior in the most basic dynamical models.

In a standard SIR model formulation, the system is divided into three classes: Susceptible (S), Infected (I) and Recovered (R). Applied to infectious diseases where waning immunity can happen, and assuming that the transmission of the disease occurs from person to person, susceptible individuals become infected and infectious, and recover after a waning immunity period. These simple epidemiological models developed to describe, for example, childhood diseases with extremely high infection rates and moderate seasonal forcing, generate Feigenbaum sequences of period-doubling bifurcations transitioning into chaos [1]. Nevertheless, different extensions of the classical SIR model applied to infectious diseases with much lower forces of infection, such as dengue fever, have also shown complex dynamics such as

* Corresponding authors.
E-mail addresses: vsteindorf@bcamath.org (V. Steindorf), asrivastav@bcamath.org (A.K. Srivastav), nstollenwerk@bcamath.org (N. Stollenwerk), bob.kooi@vu.nl (B.W. Kooi), maguiar@bcamath.org (M. Aguiar).
[1] All authors have contributed equally to this work.

https://doi.org/10.1016/j.chaos.2022.112709
Received 27 July 2022; Received in revised form 1 September 2022; Accepted 14 September 2022
Available online 3 October 2022

critical fluctuations with power-law distributions of disease cases [2], and deterministic chaos even without considering external forces such as seasonality [3,4].

Dengue fever is a viral mosquito-borne disease, a major international public health concern. The disease is transmitted by the female domestic Aedes mosquitoes, which are also vectors for yellow fever, Chikungunya and Zika viruses. With more than 3.5 billion people at risk of acquiring the infection, it is estimated that around 400 million dengue infections occur every year, of which approximately 100 million manifest symptoms with any level of disease severity [5]. Caused by four antigenic related but distinct serotypes (DENV-1 to DENV-4), infection by one serotype confers life-long immunity to that serotype, and a period of temporary cross-immunity (TCI) to other serotypes. Dengue infection shows a wide spectrum of clinical presentations, from asymptomatic to severe cases. While primary infections are often benign, with most patients experiencing a self-limiting non-severe clinical course of infection, the secondary infection with a non-identical serotype will eventually progress to severe disease characterized by hemorrhagic symptoms, via the so-called Antibody-Dependent Enhancement (ADE) process [6–9].

Mathematical models describing dengue fever epidemiological dynamics are found back from 1970 [10]. A careful review of dengue modeling framework was recently published [11], where three structural approaches were studied, the within-host, the vector–host, and the host-to-host transmission models. While the within-host framework is built to describe viral replication and immunological responses affecting differently disease outcomes in primary and secondary infections, see e.g. [12,13], the other two approaches aim to describe disease transmission at population level. The vector–host approach considers the explicit dynamics for the mosquito population affecting the disease transmission dynamics, whereas the host-to-host approach includes the effect of seasonality to mimic the mosquito dynamics, see e.g. [14,15], essential to explain the yearly dengue outbreaks.

Several mathematical models describing the transmission of dengue viruses have been proposed to explain the irregular behavior of disease epidemics. Extended SIR type models including biological features related to dengue epidemiology, such as TCI and ADE, have shown chaotic behavior in wider parameter regions [3,4,14–18], opening new ways to analyze the available incidence data. Although the complexity of these models is dependent on the number of components included in the framework, the extent of biological mechanisms generating complex behavior in simple epidemiological models is still unexplored.

In this paper, we study a basic SIR–SIR type model, a simplified version to previously proposed multi-strain models for dengue fever in which deterministic chaos was found in an unexpected and more biological parameter regions [3,14]. Without considering strain structure of pathogens, the model captures differences between primary and secondary infections, and includes two important biological features, the temporary immunity after a primary infection, analogous to the well-known temporary cross-immunity period described in dengue epidemiology, and disease enhancement in subsequent infections, analogous to the ADE effect occurring in secondary dengue infections.

Aiming to identify to which extent these biological mechanisms can generate complex behavior in simple epidemiological models, three scenarios of temporary immunity occurring after primary infection are investigated. We consider short, medium and long immunity periods, combined with different values of disease enhancement factor on secondary infections, smaller than 1, i.e. with secondary infection contributing to the overall force of infection less than the primary infection, or larger than 1, otherwise. Stability analysis of the system is performed using the classical linearization theory, and the qualitative behavior of the model is investigated with a detailed bifurcation analysis. Results presented here are of use to understand the role of biological features of infectious diseases epidemiology characterized by complex dynamics.

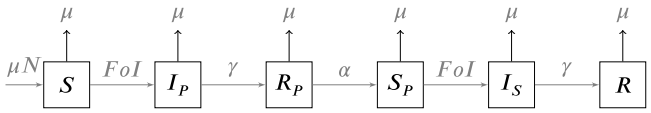

Fig. 1. Flowchart for the two infection SIR compartmental model. With demographic rate μ, infection rate β, and recovery rate γ, the Force of Infection (FoI) is given by $\beta(I_P + \phi I_S)/N$.

The paper is structured as follows. The mathematical model is formulated and described in Section 2. The qualitative analysis of the model is investigated is Sections 3 and 4. A detailed numerical bifurcation analysis, followed by numerical experiments showing complex dynamics is carried out in Section 5, and in Section 6, seasonality is considered. Finally, the discussion and conclusion remarks are presented in Section 7.

2. The two-infection model without pathogen structure

Motivated by dengue fever epidemiology, the proposed model is a simplified version of the multi-strain dengue model proposed in [3,14]. Without strain structure of the pathogens, the two infection SIR–SIR model divides the population into 6 classes: susceptible without a previous infection (seronegative S), infected for the first time (I_P), recovered from the first infection (R_P), susceptible with a previous infection (seropositive S_P), infected for the second time (I_S) and recovered from the second infection (R). The model captures differences between primary and secondary infections, and includes two important features described in dengue fever epidemiology, the temporary immunity after a primary infection and disease enhancement in a subsequent infection, see Fig. 1.

The temporary immunity refers to the progressive loss of pre-existing protective antibodies, i.e. waning immunity period parametrized by α, analogous to the well known temporary cross-immunity (TCI) period in dengue fever epidemiology. Moreover, with epidemiological studies supporting the association of severe disease with secondary dengue infection, due to the antibody-dependent enhancement (ADE) process, we assume that experiencing a first infection plays a role on disease severity. Therefore, a disease enhancement feature, parametrized by ϕ, is considered. The parameter ϕ is a scaling factor used to differentiate the baseline infectivity β of primary infection with respect to the infectivity $\phi\beta$ of secondary infections. The value of ϕ can be tuned to reflect different situations. A value of $\phi > 1$ acts increasing the infectivity of secondary infection, due to the level immunity created by the primary infection, leading to asymptomatic/mild disease manifestation, and hence higher mobility and possibility of interactions. However, a value of $\phi < 1$ indicates that individuals experiencing a secondary severe infection will contribute less to the spread of the infection. The last assumption is based on the ADE process, where the pre-existing antibodies to a previous infection do not neutralize but rather enhance the growth rate of the new viral strain, generating severe symptoms, and hence leading to hospitalization, decreasing the mobility and possibility of interactions. If $\phi = 1$, there is no protection nor enhancement, thus the secondary infected individuals transmit the disease as much as individuals in its first infection.

The flowchart of the minimalistic two infection dengue model is shown in Fig. 1, and the complete system of ordinary differential equations is given by

$$\frac{dS}{dt} = -\frac{\beta}{N}S(I_P + \phi I_S) + \mu(N - S) \tag{1a}$$
$$\frac{dI_P}{dt} = \frac{\beta}{N}S(I_P + \phi I_S) - (\gamma + \mu)I_P \tag{1b}$$
$$\frac{dR_P}{dt} = \gamma I_P - (\alpha + \mu)R_P \tag{1c}$$
$$\frac{dS_P}{dt} = -\frac{\beta}{N}S_P(I_P + \phi I_S) + \alpha R_P - \mu S_P \tag{1d}$$
$$\frac{dI_S}{dt} = \frac{\beta}{N}S_P(I_P + \phi I_S) - (\gamma + \mu)I_S \tag{1e}$$
$$\frac{dR}{dt} = \gamma I_S - \mu R\,. \tag{1f}$$

The dynamic of the model is described as follows. Susceptible (S) individuals become infected for the first time (I_P) and transmit the disease with infection rate β. They recover from the first infection (R_P), and after a period of temporary cross-immunity α, become susceptible again (S_P). Having experienced a previous dengue infection, individuals can be infected for the second time (I_S), transmitting the disease with infection rate $\phi\beta$. Susceptible individuals can acquire the infection either from individuals in a primary or secondary infection, and hence, the force of infection is given explicitly by $\beta I_P + \phi\beta I_S$. Individuals in a secondary infection recovers (R) with recovery rate γ.

For the sake of simplicity, we assume natural mortality and birth rates to be equal for all individuals, independent of the disease state, with the following dynamics for the total population $\frac{dN}{dt} = 0$ satisfied. With a constant population size $N = S + S_P + R_P + I_P + I_S + R$, the dynamic for the recovered individuals is simple

$$R = N - (S + S_P + R_P + I_P + I_S),$$

and the Equation System (1) can be reduced to an equivalent five dimensional system shown in Equation System (2)

$$\frac{dS}{dt} = -\frac{\beta}{N}S(I_P + \phi I_S) + \mu(N - S) \tag{2a}$$
$$\frac{dI_P}{dt} = \frac{\beta}{N}S(I_P + \phi I_S) - (\gamma + \mu)I_P \tag{2b}$$
$$\frac{dR_P}{dt} = \gamma I_P - (\alpha + \mu)R_P \tag{2c}$$
$$\frac{dS_P}{dt} = -\frac{\beta}{N}S_P(I_P + \phi I_S) + \alpha R_P - \mu S_P \tag{2d}$$
$$\frac{dI_S}{dt} = \frac{\beta}{N}S_P(I_P + \phi I_S) - (\gamma + \mu)I_S\,. \tag{2e}$$

3. Equilibria and stability analysis of the system

The equilibria of the system are the solutions of the following equations

$$0 = -\frac{\beta}{N}S(I_P + \phi I_S) + \mu(N - S) \tag{3a}$$
$$0 = \mu(N - S) - (\gamma + \mu)I_P \tag{3b}$$
$$0 = \gamma I_P - (\alpha + \mu)R_P \tag{3c}$$
$$0 = -\frac{\beta}{N}S_P(I_P + \phi I_S) + \alpha R_P - \mu S_P \tag{3d}$$
$$0 = \alpha R_P - \mu S_P - (\gamma + \mu)I_S\,. \tag{3e}$$

From Eq. (3c), we have

$$R_P = \frac{\gamma}{\alpha + \mu}I_P\,. \tag{4}$$

From Eq. (3b), we have

$$S = N - \frac{(\gamma + \mu)}{\mu}I_P\,. \tag{5}$$

From Eq. (3e), we have

$$S_P = \frac{\alpha}{\mu}R_P - \frac{(\gamma + \mu)}{\mu}I_S \tag{6}$$
$$= \frac{\alpha\gamma}{\mu(\alpha + \mu)}I_P - \frac{(\gamma + \mu)}{\mu}I_S\,. \tag{7}$$

Furthermore, from Eqs. (3a) and (3d), results that

$$\frac{\mu(N - S)}{S} = \frac{\alpha R_P - \mu S_P}{S_P}\,, \tag{8}$$

and

$$S_P = \frac{\alpha R_P S}{\mu N}\,. \tag{9}$$

For the equality $I_S S = I_P S_P$, the following result holds

$$I_S = \frac{I_P S_P}{S} = I_P\frac{\alpha R_P}{\mu N} = I_P^2\frac{\alpha}{\mu N}\frac{\gamma}{\alpha + \mu}\,. \tag{10}$$

Substituting the equality described in Eq. (10) in Eq. (3a), a cubic polynomial in the variable I_P is obtained. The roots are $I_P = 0$, giving the trivial Disease Free Equilibrium (DFE) solution $E_0 = (N, 0, 0, 0, 0)^T$, and, $I_P \neq 0$ are the roots of the following quadratic polynomial

$$P(I_P) = \frac{\phi\alpha\gamma}{\alpha + \mu}(\gamma + \mu)I_P^2 + \left(\gamma + \mu - \frac{\phi\alpha\gamma}{\alpha + \mu}\right)\mu N I_P - (\mu N)^2\left(1 - \frac{\gamma + \mu}{\beta}\right)\,. \tag{11}$$

By defining

$$\tilde{\phi} = \phi\gamma\frac{\alpha}{\alpha + \mu}, \qquad \tilde{\gamma} = \gamma + \mu\,,$$

the solutions of the polynomial can be written as

$$I_{p_{(1,2)}} = (p \pm \sqrt{q})\mu N\,,$$

where

$$p = \frac{\tilde{\phi} - \tilde{\gamma}}{2\tilde{\phi}\tilde{\gamma}}, \qquad q = p^2 + \frac{1}{\tilde{\phi}\tilde{\gamma}}\left(1 - \frac{\tilde{\gamma}}{\beta}\right)\,.$$

The endemic equilibrium is defined by

$$E_1 = \left(N - \frac{(\gamma + \mu)}{\mu}I_P, I_P, \frac{\gamma}{\alpha + \mu}I_P, \frac{\alpha\gamma}{\mu(\alpha + \mu)}I_P - \frac{(\gamma + \mu)}{\mu}I_S, \frac{\alpha}{\mu N}\frac{\gamma}{\alpha + \mu}I_P^2\right)\,, \tag{12}$$

where I_{P_1} and I_{P_2} are the solutions of the quadratic polynomial shown in Eq. (11).

3.1. Basic reproduction number and epidemiological thresholds

The threshold of an epidemic is commonly referred in terms of the basic reproduction number,

$$\mathcal{R}_0,$$

defined as the average number of secondary cases generated from a primary index case, during its infectiveness before recovering in a completely susceptible population [19–23]. The basic reproduction number $\mathcal{R}_0$ measures the transmission potential of a disease. If $\mathcal{R}_0 > 1$, the number of disease cases will increase exponentially, such as at the start of an epidemic, and for $\mathcal{R}_0 < 1$, disease cases will decline towards extinction. While $\mathcal{R}_0 = 1$, the so called epidemic threshold, refers to the disease endemic scenario, mathematically, $\mathcal{R}_0 = 1$ is the value where the transcritical bifurcation occurs, i.e. the threshold value for the stability and existence of the epidemiological endemic equilibrium.

The basic reproduction number of the Equation System (1) is derived from the model parameters, giving by $\mathcal{R}_0 = \frac{\beta}{\gamma+\mu}$. Therefore, the roots of the quadratic polynomial can be rewritten as

$$I_{p_{(1,2)}} = (p \pm \sqrt{q})\mu N\,, \tag{13}$$

where

$$p = \frac{\tilde{\phi} - \tilde{\gamma}}{2\tilde{\phi}\tilde{\gamma}}, \qquad q = p^2 + \frac{1}{\tilde{\phi}\tilde{\gamma}}\left(1 - \frac{1}{\mathcal{R}_0}\right). \tag{14}$$

The existence of equilibria of the model can be formalized as follows.

Theorem 1. *The system has always a disease free equilibrium, namely* $D_0 = (N, 0, 0, 0, 0, 0)$.

Theorem 2. *If* $\mathcal{R}_0 > 1$ *the system has only one endemic equilibrium.*

Proof. In fact, if $\mathcal{R}_0 > 1$, then $q > 0$ and thus, $p < \sqrt{q}$. Therefore, it follows that the unique positive root of the polynomial $P(I_p)$ has only one positive real root, that is

$$I_P = (p + \sqrt{q})\mu N . \tag{15}$$

From this, we prove that, if $\mathcal{R}_0 > 1$, only one endemic equilibrium exists, and it is given by Eq. (12). □

Theorem 3. *If* $\mathcal{R}_0 = 1$, *then a non-trivial endemic equilibrium exists if, and only if,* $\phi > \phi_c = \frac{\alpha+\mu}{\alpha}\frac{\gamma+\mu}{\gamma}$.

Proof. In fact, if $\mathcal{R}_0 = 1$, then $q > 0$ and thus, $p = \sqrt{q}$. Therefore, it follows that

$$I_{p_1} = 0 \quad \text{and} \quad I_{p_2} = 2p = \frac{\tilde{\phi} - \tilde{\gamma}}{\tilde{\phi}\tilde{\gamma}} . \tag{16}$$

This second root, I_{p_2}, is positive only if

$$\frac{\phi\gamma\alpha}{\alpha + \mu} > \gamma + \mu, \tag{17}$$

that is, for

$$\phi > \frac{\alpha + \mu}{\alpha}\frac{\gamma + \mu}{\gamma} > 1 . \quad \square \tag{18}$$

Theorem 4. *If* $\mathcal{R}_b < \mathcal{R}_0 < 1$, *then the system has two non-trivial endemic equilibria if, and only if,* $\phi > \phi_c > 1$.

Proof. In fact, if $\mathcal{R}_0 < 1$, then $p > \sqrt{q}$. Moreover, if $\phi < \phi_c$, $\tilde{\phi} - \tilde{\gamma} < 0$. Thus, both roots of the polynomial will be negative.

On the other hand, if $\phi > \phi_c$, $\tilde{\phi} - \tilde{\gamma} > 0$. Thus, both roots will be real and positive if, and only if, $q > 0$, that is, if

$$(\tilde{\phi} - \tilde{\gamma})^2 > 4\tilde{\phi}\tilde{\gamma}(-1 + \frac{1}{\mathcal{R}_0}) , \tag{19}$$

and thus, only if

$$\mathcal{R}_0 > 4\tilde{\phi}\tilde{\gamma} - (\tilde{\phi} - \tilde{\gamma})^2 =: \mathcal{R}_b . \tag{20}$$

Therefore, the system will have two non-trivial endemic equilibria when $\mathcal{R}_b < \mathcal{R}_0 < 1$. □

The appearance of endemic equilibria at the transcritical bifurcation ($\mathcal{R}_0 = 1$) characterizes the so called backward bifurcation. The mathematical formalization of the backward bifurcation, sometimes referred as subcritical bifurcation [21], will be formalized in the next section, using the center manifold theory.

Remark 1. If $\mathcal{R}_0 = \mathcal{R}_b = 4\tilde{\phi}\tilde{\gamma} - (\tilde{\phi} - \tilde{\gamma})^2$, that is, when

$$\beta = \beta_c = \frac{\tilde{\gamma}}{4\tilde{\phi}\tilde{\gamma} - (\tilde{\phi} - \tilde{\gamma})^2} , \tag{21}$$

the two positive equilibria collide. At this value occurs the so called saddle–node (tangent) bifurcation.

Theorem 5. *If* $\mathcal{R}_0 < \mathcal{R}_b$, *then the system only has the disease free-equilibrium.*

Proof. In fact, if $\mathcal{R}_0 < \mathcal{R}_b$, then $q < 0$. Therefore, it follows that the solutions of the quadratic polynomial are conjugated complex roots. In addition, only $I_P = 0$ is a positive real solution for the cubic polynomial and, therefore, for the system. □

The results proved in the theorems above are shown in Fig. 2. Fig. 2(a) shows the case of $\mathcal{R}_0 > 1$ (with $\beta = 2\gamma$), where the system exhibits a unique positive endemic equilibrium for any value of ϕ, as described in Theorem 2. For the case of $\mathcal{R}_b < \mathcal{R}_0 < 1$ (with $\beta \approx 0.96\gamma$), the system shows two positive endemic equilibria for $\phi > \phi_c$, as described in Theorem 4, see Fig. 2(b).

3.2. Characterization of the backward bifurcation

We consider the results established in Ref. [24], related to the nature of the fixed point of the model, $x = x_0$, near to the transcritical bifurcation point, when the reproduction number $\mathcal{R}_0 = 1$, i.e. when the eigenvalue of the Jacobian matrix, evaluated at the fixed point, is zero.

For convenience, we define $S = x_1$, $I_P = x_2$, $R_P = x_3$, $S_P = x_4$ and $I_S = x_5$, and let the vector x be $x = (x_1, x_2, x_3, x_4, x_5)^T$. The system (1) is rewritten as

$$x_1' = -\frac{\beta}{N}x_1(x_2 + \phi x_5) + \mu(N - x_1) \tag{22}$$

$$x_2' = \frac{\beta}{N}x_1(x_2 + \phi x_5) - (\gamma + \mu)x_2 \tag{23}$$

$$x_3' = \gamma x_2 - (\alpha + \mu)x_3 \tag{24}$$

$$x_4' = -\frac{\beta}{N}x_4(x_2 + \phi x_5) + \alpha x_3 - \mu x_4 \tag{25}$$

$$x_5' = \frac{\beta}{N}x_4(x_2 + \phi x_5) - (\gamma + \mu)x_5 \tag{26}$$

that is,

$$\frac{dx}{dt} = (f_1, f_2, f_3, f_4, f_5)^T .$$

The theory in Ref. [24] considers a general ODE system

$$\frac{dx}{dt} = f(x, \lambda),$$

depending on the parameter λ, such that $\mathcal{R}_0 < 1$ for $\lambda < 0$, and $\mathcal{R}_0 > 1$ for $\lambda > 0$. And

$$f : \mathbb{R}^n \times \mathbb{R} \to \mathbb{R}^n, f \in \mathbb{C}^2(\mathbb{R}^n \times \mathbb{R}),$$

where x_0 is an equilibrium of the system ($f(x_0, \lambda) = 0, \ \forall\lambda$). Moreover,

1. $A = D_x f(x_0, 0) = \left(\frac{\partial f_i}{\partial x_j}(x_0, 0)\right)$ is the linearized matrix of the system at the equilibrium x_0, with f evaluated at $\lambda = 0$.
2. Zero is a simple eigenvalue of A, while the other eigenvalues of A have negative real parts.
3. Matrix A has a right w and a left v eigenvectors corresponding to the zero eigenvalues.

Considering the assumptions above, the nature of the endemic equilibria near to the bifurcation point is determined by the sign of

$$a = \sum_{k,i,j=1}^{n} v_k w_i w_j \frac{\partial^2 f_k}{\partial x_i \partial x_j}(x_0, 0) , \tag{27}$$

and

$$b = \sum_{k,i=1}^{n} v_k w_i \frac{\partial^2 f_k}{\partial x_i \partial \lambda}(x_0, 0) , \tag{28}$$

with f_k being the kth component of f, see Ref. [24].

We apply the results described above to the Equation System (3), in which the Jacobian matrix at the disease-free equilibrium $x = x_0 = (N, 0, 0, 0, 0)$ has a zero eigenvalue at $\mathcal{R}_0 = 1$, this is, when $\beta = \gamma + \mu = \beta^*$. The transmission rate β is the chosen bifurcation parameter for this analysis (since the value of $\mathcal{R}_0$ depends on this parameter).

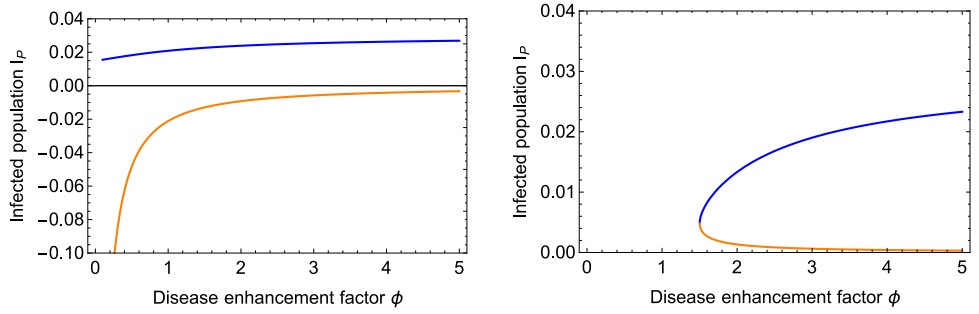

(a) $\beta = 104 = 2\gamma$ (b) $\beta = 50 \approx 0.96\gamma$

Fig. 2. Graphical presentation of the system's equilibria (primary infected population I_P). For fixed parameter values shown in Table 1, the disease enhancement factor ϕ is varying. In (a) $\beta = 2\gamma$, i.e. $\mathcal{R}_0 > 1$. Note that the negative values in (a) are not considered as a solution of the system, since it does not a have biological meaning. In (b) $\beta \approx 0.96\gamma$, i.e., $\mathcal{R}_0 < 1$.

The Jacobian matrix at $x = x_0$, with $\beta = \beta^*$, is given by

$$\mathrm{A} = \begin{pmatrix} -\mu & -\beta^* & 0 & 0 & -\beta^*\phi \\ 0 & 0 & 0 & 0 & \beta^*\phi \\ 0 & \gamma & -\alpha-\mu & 0 & 0 \\ 0 & 0 & \alpha & -\mu & 0 \\ 0 & 0 & 0 & 0 & -\beta^* \end{pmatrix}. \tag{29}$$

The matrix A has a right eigenvector (corresponding to the zero eigenvalue), given by $w = (w_1\ w_2\ w_3\ w_4\ w_5)^T$, where

$$w = \left(\tfrac{-\beta}{\mu}w_2, \quad \tfrac{\alpha+\mu}{\gamma}w_3, \quad w_3, \quad \tfrac{\alpha}{\mu}w_3, \quad 0\right)^T$$
$$= \left(\tfrac{-\beta}{\mu}(\tfrac{\alpha+\mu}{\gamma}), \quad \tfrac{\alpha+\mu}{\gamma}, \quad 1, \quad \tfrac{\alpha}{\mu}, \quad 0\right)^T.$$

The matrix A has a left eigenvector (corresponding to the zero eigenvalue), given by $v = (v_1\ v_2\ v_3\ v_4\ v_5)$, where

$$v = \left(0, \quad \tfrac{\gamma+\mu}{\beta\phi}, \quad 0, \quad 0, \quad 1\right).$$

Therefore, in this case,

$$a = v_2 \sum_{i,j=1}^{n} w_i w_j \frac{\partial^2 f_2}{\partial x_i \partial x_j}(x_0, \beta^*) + v_5 \sum_{i,j=1}^{n} w_i w_j \frac{\partial^2 f_5}{\partial x_i \partial x_j}(x_0, \beta^*)$$
$$= v_2\left(w_1 w_2 \frac{\beta}{N} + w_2 w_1 \frac{\beta}{N}\right) + v_5\left(w_2 w_4 \frac{\beta}{N} + w_4 w_2 \frac{\beta}{N}\right)$$
$$= 2\frac{\beta}{N} w_2(w_1 v_2 + w_4 v_5),$$

and thus,

$$a = 2\frac{\beta}{N}\frac{\alpha+\mu}{\gamma}\left(\frac{-\beta}{\mu}\frac{(\alpha+\mu)}{\gamma}\frac{(\gamma+\mu)}{\beta\phi} + \frac{\alpha}{\mu}\right). \tag{30}$$

For the computation of b, we have

$$b = v_2 \sum_{i=1}^{n} w_i \frac{\partial^2 f_2}{\partial x_i \partial \beta}(x_0, \beta^*) + v_5 \sum_{i=1}^{n} w_i \frac{\partial^2 f_5}{\partial x_i \partial \beta}(x_0, \beta^*)$$
$$= v_2 w_2.$$

Since, v_2 and w_2 are positive, b is always positive. Moreover, the sign of a follow these inequalities:

$$a < 0 \text{ if and only if } \phi < \frac{(\alpha+\mu)(\gamma+\mu)}{\gamma\alpha} \tag{31}$$

$$a > 0 \text{ if and only if } \phi > \frac{(\alpha+\mu)(\gamma+\mu)}{\gamma\alpha}, \tag{32}$$

establishing the result described in Ref. [24], and formalized below in Theorem 6.

Theorem 6. *The system exhibits a backward bifurcation at $\mathcal{R}_0 = 1$ if, and only if, $\phi > \phi_c = \frac{(\alpha+\mu)(\gamma+\mu)}{\gamma\alpha}$.*

Results of Theorem 6 are shown in Fig. 3. While for $\phi < \phi_c$, the transcritical bifurcation occurs at $\mathcal{R}_0 = 1$, see Fig. 3(a), the backward bifurcation occurs for $\phi > \phi_c$, see Fig. 3(b).

4. Stability of the epidemiological equilibria

The stability of equilibria of the Ordinary Differential Equation (ODE) System (1) will be analyzed via the classical linearization theory. The Jacobian matrix, at a point $E = (S, I_P, R_P, S_P, I_S)$, is given by

$$\mathrm{J(E)} = \begin{pmatrix} -\frac{\beta(I_S\phi+I_P)}{N} - \mu & -\frac{\beta S}{N} & 0 & 0 & -\frac{\beta S\phi}{N} \\ \frac{\beta(I_S\phi+I_P)}{N} & \frac{\beta S}{N} - (\gamma+\mu) & 0 & 0 & \frac{\beta S\phi}{N} \\ 0 & \gamma & -\alpha-\mu & 0 & 0 \\ 0 & -\frac{\beta S_P}{N} & \alpha & -\frac{\beta(I_S\phi+I_P)}{N} - \mu & -\frac{\beta S_P\phi}{N} \\ 0 & \frac{\beta S_P}{N} & 0 & \frac{\beta(I_S\phi+I_P)}{N} & \frac{\beta S_P\phi}{N} - (\gamma+\mu) \end{pmatrix}. \tag{33}$$

4.1. Stability of Disease Free Equilibrium (DFE)

Theorem 7. *If $\mathcal{R}_0 < 1$, then the disease free is asymptotically stable. And it is unstable when $\mathcal{R}_0 > 1$.*

Proof. The stability of the disease-free equilibrium $E_0 = (N, 0, 0, 0, 0)$ will be given by the eigenvalues of Jacobian matrix evaluated at E_0:

$$\mathrm{J(E_0)} = \begin{pmatrix} -\mu & -\beta & 0 & 0 & -\beta\phi \\ 0 & \beta-(\gamma+\mu) & 0 & 0 & \beta\phi \\ 0 & \gamma & -\alpha-\mu & 0 & 0 \\ 0 & 0 & \alpha & -\mu & 0 \\ 0 & 0 & 0 & 0 & -(\gamma+\mu) \end{pmatrix}. \tag{34}$$

The eigenvalues of the Jacobian matrix $J(E_0)$ given in Eq. (34) are given by

$$\lambda_1 = -\mu$$
$$\lambda_2 = -(\gamma+\mu)(1-\mathcal{R}_0)$$
$$\lambda_3 = -(\alpha+\mu)$$
$$\lambda_4 = -\mu$$
$$\lambda_5 = -(\gamma+\mu),$$

with all the eigenvalues being negative, except for λ_2. However, if $\mathcal{R}_0 < 1$, then $\beta - (\gamma+\mu) < 0$, and all the eigenvalues are negative. □

4.2. Stability of Disease Endemic Equilibrium (DEE)

The stability of the DEE will be given by the eigenvalues of Jacobian matrix evaluated at E_1.

Theorem 8. *The endemic equilibrium*

$$E_1 = \left(N - \frac{(\gamma+\mu)}{\mu}I_P, I_P, \frac{\gamma}{\alpha+\mu}I_P, \frac{\alpha\gamma}{\mu(\alpha+\mu)}I_P\right.$$
$$\left. -\frac{(\gamma+\mu)}{\mu}\left(\frac{\alpha}{\mu N}\frac{\gamma}{\alpha+\mu}\right)I_P^2, \frac{\alpha}{\mu N}\frac{\gamma}{\alpha+\mu}I_P^2\right)$$

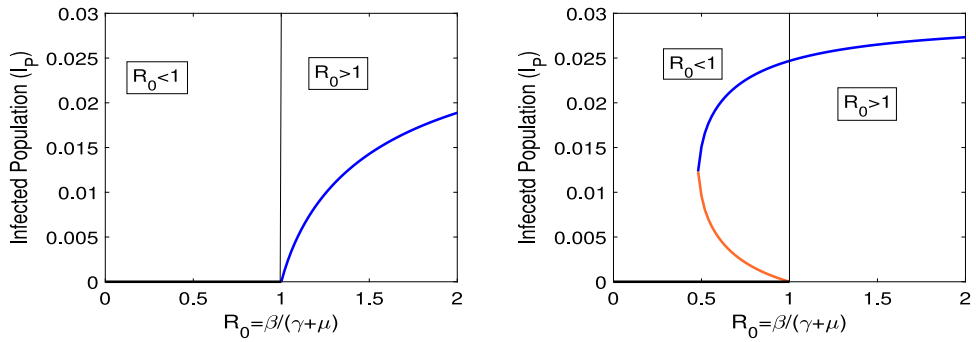

(a) Transcritical bifurcation for $\phi = 0.5$ (b) Backward bifurcation for $\phi = 1.5$

Fig. 3. Graphical presentation for the system's equilibria (infected population I_P) when $\mathcal{R}_0$ is varying. For fixed parameter values shown in Table 1, the infection rate parameter β is varying. In (a) $\phi = 0.6 < \phi_c$, and in (b) $\phi = 1.5 > \phi_c$. The black line represents the disease free equilibrium and the blue and orange lines represent the endemic equilibrium. Note that in (b) while the blue line represents the upper branch of the endemic equilibrium, the orange line represents the lower branch of the endemic equilibrium. (For interpretation of the references to color in this figure legend, the reader is referred to the web version of this article.)

is locally asymptotically stable if the coefficients of the characteristic polynomial satisfies the Routh–Hurwitz criteria (see Appendix A), otherwise it is unstable.

Proof. The Jacobian matrix evaluated at E_1 is given by

$$J(E_1) = \begin{pmatrix} -a_{11} & -a_{12} & 0 & 0 & -a_{15} \\ a_{21} & a_{22} & 0 & 0 & a_{25} \\ 0 & \gamma & -\alpha-\mu & 0 & 0 \\ 0 & -a_{42} & \alpha & -a_{44} & -a_{45} \\ 0 & a_{52} & 0 & a_{54} & a_{55} \end{pmatrix}, \tag{35}$$

where

$$a_{11} = \frac{\beta(I_s\phi + I_P)}{N} - \mu, a_{12} = \frac{\beta S}{N}, a_{15} = \frac{\beta S\phi}{N}$$

$$a_{21} = \frac{\beta(I_S\phi + I_P)}{N}, a_{22} = \frac{\beta S}{N} - \gamma - \mu, a_{25} = \frac{\beta S\phi}{N},$$
$$a_{42} = \frac{\beta S_P}{N}, a_{44} = \frac{\beta(I_S\phi + I_P)}{N} - \mu$$

$$a_{45} = \frac{\beta S_P\phi}{N}, a_{52} = \frac{\beta S_P}{N}, a_{54} = \frac{\beta(I_S\phi + I_P)}{N}, a_{55} = \frac{\beta S_P\phi}{N} - \gamma - \mu.$$

Therefore, the characteristic polynomial is given by

$$Q(\lambda) = \lambda^5 + G_1\lambda^4 + G_2\lambda^3 + G_3\lambda^2 + G_4\lambda + G_5, \tag{36}$$

where the coefficients are

$$\begin{aligned}
G_1 &= a_{22} - a_{11} + a_{55} - a_{44} - \alpha - \mu \\
G_2 &= a_{55}(a_{44} + \alpha + \mu) - a_{44}(\alpha + \mu) - a_{54}a_{45} \\
&\quad - (a_{22} - a_{11})(a_{55} - a_{44} - \alpha - \mu) \\
&\quad + a_{11}a_{22} - a_{21}a_{12} \\
G_3 &= (\alpha + \mu)(a_{55}a_{44} - a_{45}a_{54}) - (a_{55} - a_{44} - \alpha - \mu)a_{11}a_{22} + a_{25}a_{55}(\gamma - a_{42}) \\
&\quad - [a_{55}(a_{44} + \alpha + \mu) - a_{44}(\alpha + \mu) - a_{54}a_{45}](a_{22} - a_{11}) \\
&\quad + (a_{55} - a_{44} - \alpha - \mu)a_{21}a_{12} \\
G_4 &= [a_{55}(a_{44} + \alpha + \mu) - a_{44}(\alpha + \mu) - a_{54}a_{45}](a_{22}a_{11} + a_{21}a_{12}) \\
&\quad + (\alpha + \mu)(a_{55}a_{44} - a_{45}a_{54})(a_{22} - a_{11}) \\
&\quad + a_{54}a_{25}[\gamma\alpha + \gamma a_{44} - a_{42}(\alpha + \mu)] + a_{54}a_{25}[a_{54}(\gamma - a_{42})a_{11}] \\
&\quad - a_{54}(\gamma - a_{42})a_{21}a_{15} \\
G_5 &= (\alpha + \mu)(a_{55}a_{44} - a_{45}a_{54})(a_{22}a_{11} + a_{12}a_{21}) \\
&\quad + a_{54}[\gamma\alpha + \gamma a_{44} - a_{42}(\alpha + \mu)](a_{11}a_{25} - a_{21}a_{15}) .
\end{aligned}$$

Using the Routh–Hurwitz criteria, $Q(\lambda)$ will either have negative roots or roots with a negative real part if, and only if, $detH_i > 0$, with $i = 1, 2, 3, 4, 5$. The Routh–Hurwitz criteria are reduced into the following conditions

$$G_i > 0, i = 1, 2, 3, 4, 5 \tag{37}$$

$$G_1G_2G_3 > G_3^2 + G_1^2G_4 \tag{38}$$

$$(G_1G_4 - G_5)(G_1G_2G_3 - G_3^2 - G_1^2G_4) > G_5(G_1G_2 - G_3)^2 + G_1G_5^2 , \tag{39}$$

and if these three conditions are satisfied, then E_1 is stable. The Routh–Hurwitz criteria and the definition of matrix H_i can be found in Appendix A of this manuscript. □

Table 1
Baseline parameter values used for simulations. The parameter values were obtained from Refs. [3,4,14]. Note that in the following, parameters values are giving without stating explicitly the biological units, e.g, $\alpha = 2 =: \alpha = 2y^{-1}$. That holds for the following parameters: μ, γ, α and β.

Parameter	Description	Values	Unity
N	Population size	100	
μ	Birth and death rates	1/65	y^{-1}
γ	Recovery rate	52	y^{-1}
α	Temporary immunity period	2	y^{-1}
$\beta = \beta_0$	Infection rate	104	y^{-1}
ϕ	Ratio of secondary infections contribution to the overall force of infection	2.6	

The conditions described in Theorem 8 are complex analytical expressions of the model parameters. Hopf bifurcation could be found, however to give the analytical conditions are even more difficult. Instead, we use numerical methods to identify more complex bifurcations structures as presented in the next section.

5. Numerical experiments

Using the baseline parameter values shown in Table 1, numerical simulations are performed with the software AUTO [25,26], MATCONT [27], *Matlab* [28], and *Wolfram Mathematica* [29].

5.1. Numerical bifurcation analysis

A detailed numerical bifurcation analysis is performed using the software AUTO and MATCONT. Fig. 4 shows the 2-Dimensional (2D) bifurcation diagrams for different values of temporary immunity α. Two important biological parameters, the infection rate β and the disease enhancement factor ϕ are varied.

The 2D bifurcation diagram for $\alpha = 52$ is shown in Fig. 4(a). In this scenario, the temporary immunity period is very short, lasting only 7 days. The assumption of having the immunity period to last as long as the recovery period means, biologically, that infected individuals are able to acquire a second infection soon after they recover from the

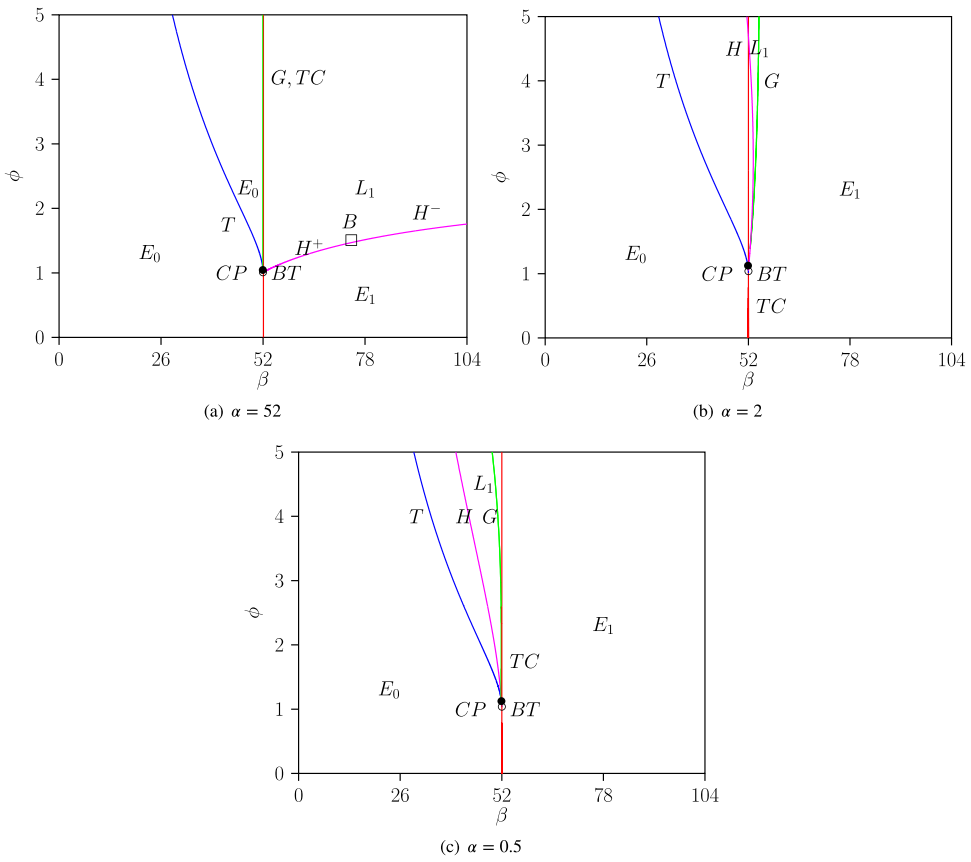

Fig. 4. 2D bifurcation diagram. Two biological parameters are varied, the infection rate parameter β, and the disease enhancement parameter ϕ. In (a) $\alpha = 52$, in (b) $\alpha = 2$ and in (c) $\alpha = 0.5$. The other parameters values are fixed as shown in Table 1. Tangent T, Transcritical TC, and Hopf H bifurcation curves are shown in blue, red and purple, respectively. E_0 and E_1 represents the stable DFE and DEE, respectively, and L_1 the stable limit cycle. CP, BT and B refers to the cusp, Bogdanov–Takens and Bautin bifurcation points, respectively. For bifurcation definitions, see Table 2. (For interpretation of the references to color in this figure legend, the reader is referred to the web version of this article.)

primary infection. In that case, the transcritical bifurcation occurs at $\mathcal{R}_0 = 1$, for $\phi < 1$. If disease enhancement is not considered, a backward bifurcation does not occur, and therefore, only the DFE is observed for $\mathcal{R}_0 < 1$.

A backward bifurcation occurs if, and only if, $\phi > \phi_c > 1$. The Hopf bifurcation occurs after the transcritical bifurcation, with the endemic equilibria becoming unstable after the H point. In this case of short immunity scenario, periodic solutions (limit cycles) are observed for higher force of infection and higher disease enhancement factor, i.e., when the contribution of secondary infection to the overall force of infection is much higher than the contribution of primary infections.

The 2D bifurcation diagram for $\alpha = 2$ is shown in Fig. 4(b). In this scenario, the temporary immunity period is longer, lasting for 6 months, as proposed in Refs. [3,14]. Here, after recovering from a primary infection, individuals are protected against a new infection for at least 6 months. Note that, biologically, it would be unlikely to observe secondary dengue infections occurring at a spacing of less than a year, since, besides the temporary immunity period, the disease transmission is highly seasonal. Similarly as described for the case of $\alpha = 52$, backward bifurcation occurs if, and only if, $\phi > \phi_c > 1$. However, although the Hopf bifurcation curve also appears after the transcritical bifurcation, in this scenario the endemic equilibria becomes stable (instead of being unstable as observed for the scenario of $\alpha = 52$) after H point.

Finally, we present the results for an even longer temporary immunity period, which is biologically closely related to dengue epidemiology, $\alpha = 0.5$. In this scenario, after recovering from a primary infection, individuals are protected against a new infection for at least 2 years. The Hopf bifurcation curve appears before the transcritical bifurcation, see Fig. 4(c). Bi-stability is observed when the backward bifurcation occurs, with a stable upper branch after the H bifurcation curve. The endemic equilibrium is stable for a small set of parameters, delimited by the Hopf (purple line) and transcritical (red line) bifurcation curves, and hence, both the DFE and the endemic equilibrium are stable before the epidemiological threshold of $\mathcal{R}_0 = 1$. That means that disease will persist even in the subcritical regime of disease transmission, when $\mathcal{R}_0 < 1$.

As a complementary analysis, we calculate numerically the eigenvalues of each endemic equilibrium, plotting the real part of the eigenvalue in function of the infection rate β. The real part of eigenvalues for each endemic equilibrium, using the same color code as presented in Fig. 3(b), are shown in Fig. 5.

For the scenario of $\alpha = 52$, see Fig. 5(a), the positive endemic equilibria is always unstable after the Hopf H bifurcation (blue line), which is the opposite dynamics as the dynamics observed for the other two scenarios of longer temporary immunity, $\alpha = 0.5$ and $\alpha = 2$. In addition, a Bautin B bifurcation point occurs at $\beta \approx 78$, i.e. $\mathcal{R}_0 = 1.5$, see Fig. 4(a), with a supercritical Hopf bifurcation H^+ identified before the B critical point. In agreement with the results shown in Fig. 5(a), a stable limit cycle is identified near to the unstable equilibrium.

For the scenario of $\alpha = 2$, see Fig. 5(b), the Hopf bifurcation H occurs after the transcritical TC bifurcation, with a unique endemic equilibrium (upper branch) changing stability, from unstable to stable (see blue line).

Bi-stability occurs only for the scenario of $\alpha = 0.5$, see Fig. 5(c). Here, the backward bifurcation occurs with two positive endemic branches. While the lower branch is always unstable (see orange line), the upper branch changes stability at $\beta \approx 49$, from unstable to stable

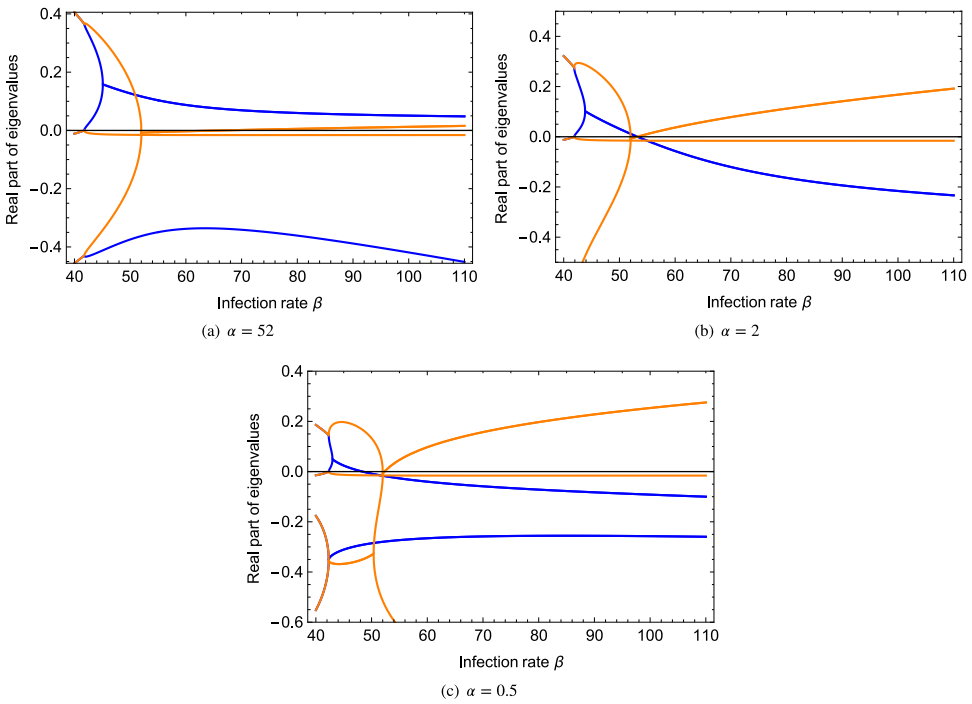

Fig. 5. The real part of the eigenvalues for the upper (blue line) and lower (orange line) branches of the endemic equilibria are shown for different temporary immunity (α) period. In (a) $\alpha = 52$, in (b) $\alpha = 2$, and in (c) $\alpha = 0.5$. The disease enhancement parameter is fixed to $\phi = 2.6$ and the infection rate β and, consequently, the $\mathcal{R}_0$ are varied. Note that close to the critical point, for $\beta = 52$, i.e. $\mathcal{R}_0 > 1$, only the upper branch of the endemic equilibrium is positive, and hence, only the eigenvalues shown in the blue line are taken into account to discuss the stability of the equilibrium. The eigenvalues were obtained using the software Wolfram Mathematica. (For interpretation of the references to color in this figure legend, the reader is referred to the web version of this article.)

after undergoing through the Hopf H bifurcation that occurs before transcritical bifurcation (see blue line).

5.2. Long time behavior of the solutions close to the transcritical bifurcation

To show the asymptotic behavior of the solutions of the system close to the transcritical bifurcation, and in agreement with the numerical results presented in Section 5.1, time series simulations are shown in Figs. 6–8. For time series simulations close to the bifurcation points see Appendix B. The three scenarios of temporary immunity are evaluated for varying values of β close to the transcritical bifurcation point (occurring at $\beta = 52.015$, i.e., for $\mathcal{R}_0 = 1$). The numerical simulations were perform with the Runge–Kutta method in Matlab software, considering a very small time step ($\Delta t = 0.001$). Using the parameter values shown in Table 1, the following initial conditions were used: $I_{t_o} = [S_0, I_{P_0}, R_{P_0}, S_{P_0}, I_{S_0}, R_0] = [45.7, 1.63, 0.01, 24.07, 0.08, 28.51]$.[2]

Fig. 6 shows the dynamical behavior obtained when temporary immunity is very short, $\alpha = 52$. In agreement with Figs. 4(a) and 5(a), the following dynamics are observed. For $\beta = \gamma = 52$, i.e. just before the transcritical TC bifurcation point, the solution converges to the disease free equilibrium, see Fig. 6(a). For $\beta = 53$, the solution oscillates with very long period length, agreeing well with the observation of the global homoclinic bifurcation, see Fig. 6(b). Finally, for $\beta = 54$, i.e. after the Hopf H bifurcation point, the endemic equilibrium is unstable, and periodic solutions are observed, see Fig. 6(c). In this case, one can conclude that the Hopf bifurcation is supercritical (H^+), and the limit cycle is stable, before Bautin bifurcation.

Fig. 7 shows the dynamical behavior obtained when temporary immunity is intermediate, $\alpha = 2$. In agreement with Figs. 4(b) and 5(b), the following dynamics are observed. For $\beta = \gamma = 52$, i.e. just before TC point, the solution converges to the disease free equilibrium, see Fig. 7(a). For $\beta = 53$, i.e., close to the H and after the TC bifurcation curves, the solution oscillates and converges to a limit cycle, see Fig. 7(b). Finally, for $\beta = 54$, after the H bifurcation curve, the endemic equilibrium is stable, see Fig. 7(c). In this case, similarly to the case of $\alpha = 52$, the Hopf bifurcation is supercritical and the limit cycle is stable, since the solution is periodic for values which are very close to H, see Fig. 7(b).

Fig. 8 shows the dynamical behavior obtained for a longer immunity period, $\alpha = 0.5$. In agreement with Fig. 4(c) and Fig. 5(c), the following dynamics are observed. For $\beta = \gamma = 48$, i.e. before the H curve, the solution oscillates and rapidly decreases, converging to the disease free equilibrium, see Fig. 8(a). For $\beta = 51$, i.e., immediately after H point, and still before TC, the solution converges to the endemic equilibrium, which is stable, see Fig. 8(b). Here, for the case of $R_0 < 1$, the endemic equilibrium is stable together with the disease-free equilibrium, and thus, bi-stability occurs, see Figs. 8(b) and 5(c). Finally, for $\beta = 53$, i.e., after the TC, we observe a stable endemic equilibrium, see Fig. 8(c). In this case, one can conclude that the Hopf bifurcation is subcritical (H^-), and the limit cycle is unstable, with oscillations occurring but not kept for longer, converging to the stable DFE, see Fig. 8(a).

6. Deterministic chaos in the simple epidemiological model

Despite incorporation of TCI in rather complicated models, the ADE effect would often been assumed to increase the transmissibility or susceptibility of individuals experiencing secondary infections [16,17,30–33]. Conversely, the modeling framework proposed by Aguiar et al. see e.g., Refs. [14,15,34], has assumed the ADE effect to rather

[2] Numerical simulations can be also obtained with the *ODE45* method from Matlab, however, the positiveness constraint is necessary to be included in order to generate results agreeing with the analytical calculations. The system is positive invariant in the first quadrant, and the solutions need to be positive for biological meaning.

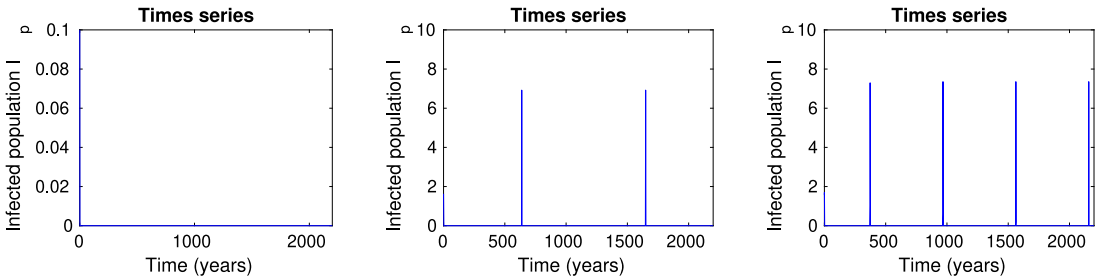

(a) $\beta = 52 = 1\gamma$ (b) $\beta = 53 \approx 1.02\gamma$ (c) $\beta = 54 \approx 1.04\gamma$

Fig. 6. Times series for fixed $\alpha = 52$, $\phi = 2.6$, and different β values close to the transcritical bifurcation point TC, i.e., for $\mathcal{R}_0 \approx 1$. In (a) $\beta = 52$, in (b) $\beta = 53$ and in (c) $\beta = 54$.

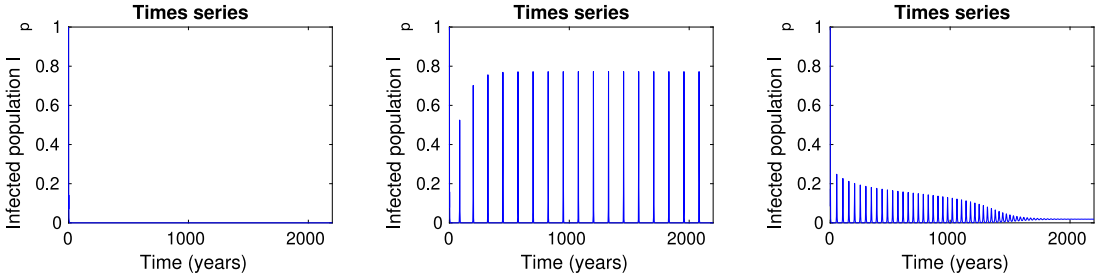

(a) $\beta = 52 = 1\gamma$ (b) $\beta = 53 \approx 1.02\gamma$ (c) $\beta = 54 \approx 1.04\gamma$

Fig. 7. Times series for fixed $\alpha = 2$, $\phi = 2.6$, and different β values close to TC point. In (a) $\beta = 52$, in (b) $\beta = 53$ and in (c) $\beta = 54$.

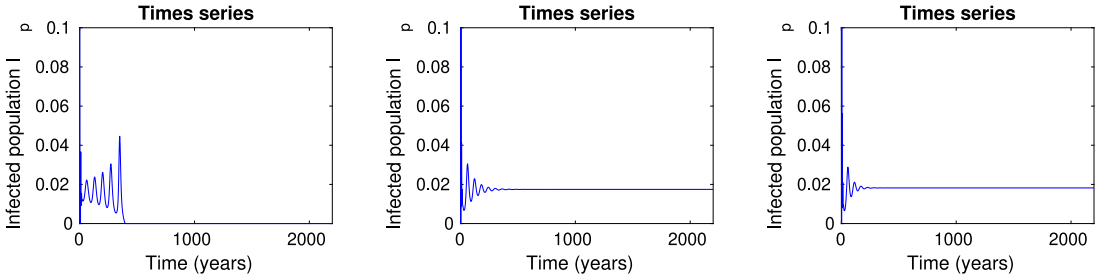

(a) $\beta = 48 \approx 0.92\gamma$ (b) $\beta = 51 \approx 0.98\gamma$ (c) $\beta = 53 \approx 1.02\gamma$

Fig. 8. Times series for fixed $\alpha = 0.5$, $\phi = 2.6$, and different β values close to the TC point. In (a) $\beta = 48$, in (b) $\beta = 51$ and in (c) $\beta = 53$.

reduce the transmissibility of individuals experiencing secondary infection, due to hospitalization of severe cases. With the constraint of secondary infection only possible to occur with a different serotype to the one causing the primary infection, the TCI was introduced through additional compartments for individuals recovering from a primary infection, becoming susceptible again after a short cross-immunity period. The combination of TCI period and ADE has shown, for the first time, a new chaotic window in an unexpected and much wider parameter regions [3]. This finding indicates that deterministic chaos is much more important in epidemiological models than previously thought. The addition of seasonality into this basic two-strain model, a cosine function included in the force of infection to mimic the fluctuations in mosquito population, led to a successful description of the empirical outbreak data [14], able to evaluate the impact of newly licensed dengue vaccine administration [35].

In this work, we study the dynamical behavior of simple two-infection SIR–SIR type model, a minimalistic version of the model proposed in Ref. [3], showing that, without seasonality, the combination of temporary immunity and disease enhancement generates a rich dynamical behavior, with several bifurcation structures being identified. In addition, the transcritical TC and the Hopf H bifurcations, tangent (saddle–node) T, global homoclinic G, Bogdanov–Takens BT, cusp CP, and Bautin B bifurcations were found, see Table 2.

Chaotic behavior is observed when seasonal forcing is included into the System (1), simply by adding a cosine function into the transmission rate β parameter, $\beta = \beta(t) = \beta_0(1 + \eta cos(\omega t))$, as proposed in Ref. [14] to mimic the fluctuations in mosquito population.

Times series and phase space plots for the non seasonal and the seasonal SIR–SIR model are shown in Figs. 9 and 10, respectively. With fixed disease enhancement $\phi = 2.6$, the dynamics for different values of temporary immunity α is compared.

For the non seasonal model, i.e., for $\beta = 104 = 2\gamma$ ($\mathcal{R}_0 \approx 2$, as suggested in Ref. [3,14]), limit cycle are only observed for short immunity period, $\alpha = 52$, when high disease enhancement is assumed ($\phi = 2.6$), see Fig. 9(a), while for an intermediate and a long immunity periods, $\alpha = 2$ and $\alpha = 0.5$, respectively, fixed point is the final solution, see Figs. 9 (b), (c) and (d). The addition of seasonality into the model, i.e., for $\beta = \beta_0 = 104 = 2\gamma$, shows irregular oscillations reassembling chaotic dynamics for higher disease enhancement, $\phi \gg 1$. Note that chaotic behavior is observed for a short immunity period ($\alpha = 52$), as well as for the long immunity period ($\alpha = 0.5$) and high enhancement factor $\phi = 5$, see Figs. 10 (a) and (d). For an intermediate immunity period ($\alpha = 2$) only periodic oscillations are observed, see Figs. 10 (b) and (c).

In addition, bifurcation diagrams for the non seasonal and the seasonal models are compared, see Figs. 11, 12, and 13, for the three scenarios of temporary immunity period. By fixing $\mathcal{R}_0 = 2$ (i.e. $\beta = 104$), the disease enhancement factor ϕ is the bifurcation parameter. Chaotic behavior is confirmed by the Lyapunov exponents calculation, and only identified to occur when seasonality is incorporated into the system.

Table 2
List of bifurcation structures identified in the two-infection SIR dengue model shown in Equation System (1).

Representation	Bifurcation	Codim[a]	Description
TC	Transcritical	1	One zero eigenvalue, exchange of stability between two equilibria (DFE and DEE)
T	Tangent	1	One zero eigenvalue, collision of two equilibria (DEE)
H	Hopf	1	Pair of conjugated complex eigenvalues with zero real part, equilibrium (DEE) becomes unstable, origin of limit cycle
G	Global homoclinic	1	Disappearance of limit cycle, collision with equilibrium
BT	Bogdanov–Takens	2	Equilibrium has two zero eigenvalues
CP	Cusp	2	Equilibrium (DFE) one simple zero eigenvalue transcritical bifurcation changes criticality
B	Bautin	2	Hopf bifurcation changes criticality (from supercritical to subcritical), origin of tangent to limit cycle

[a]The co-dimension (codim) of a bifurcation refers to the number of parameters which must be varied for the bifurcation to occur.

For the non seasonal system, a Hopf bifurcation occurs when short immunity period and high disease enhancement is assumed, while for the intermediate and long immunity periods, fixed point is observed, see Fig. 11. Note that, the addition of the seasonal term transform the autonomous ODE (AODE) system into a non-autonomous system (NODE), with both, the trajectory and the stability concepts been time dependent [37].

Regarding the calculation of the spectrum of Lyapunov exponents, while the AODE system has a zero Lyapunov exponent, for the NODE system, the zero Lyapunov exponent of the limit cycle does not generally occur, since it is in the seasonal forcing. The classical interpretation of dynamical attractors from Lyapunov spectra for forced as for unforced systems is equal when using the Hopf-oscillator-subsystem for the forcing, with the benefit that we have an autonomous system with the limit cycle showing the zero Lyapunov exponent. In the current non-autonomous system, the classification of the dynamical attractors are given as follows: limit cycles having negative dominant nontrivial Lyapunov exponent, torus having zero dominant non-trivial Lyapunov exponent and chaotic attractors having positive dominant non-trivial Lyapunov exponent [3,36].

For the seasonal model, i.e., non-autonomous system, chaotic behavior is found for both, short immunity period ($\alpha = 52$), see Fig. 12(a) and (c), and long immunity period ($\alpha = 0.5$), see Fig. 13, but always restricted to a high disease enhancement factor of $\phi > 1$. For an intermediate immunity period ($\alpha = 2$), only the limit cycle from the seasonal forcing is appearing in the relevant parameter region, see see Fig. 12(b) and (d).

7. Discussion and conclusions

The development of mathematical tolls to guide public health authorities for disease prevention and control in different epidemiological scenarios is a major challenge. Consideration of the intrinsic dynamical behavior and the limitations of the so far existing modeling frameworks are crucial for the successful interpretation of the results. However, modeling insights for epidemiological scenarios characterized by complex dynamics are still to be described.

In this paper, we study a two infection SIR–SIR model, motivated by dengue epidemiology, the minimalistic version of the model proposed by Aguiar et al. in Refs. [3,14], in which deterministic chaos was found in wider parameter regions. Without considering strain structure of pathogens, our model captures differences between primary and secondary infections, and includes two important biological features, the temporary immunity after a primary infection, analogous to the well-known temporary cross-immunity period described in dengue epidemiology, and disease enhancement in subsequent infections, analogous to the ADE effect occurring in secondary dengue infections.

Although the complexity of these models is dependent on the number of components and the temporal resolution, the mechanisms described by Aguiar et al. [3,4,14,18] are likely to be present in other diseases caused by multiple strains where complex dynamics can eventually be observed in a more simple framework. The extent of biological mechanisms generating complex behavior in simple epidemiological models is still unexplored.

Aiming to investigate to what extent the well known biological features of dengue epidemiology, TCI and ADE, are needed to generate complex dynamics in simple epidemiological models, without the addition of external forces such as seasonality. Three scenarios of temporary immunity occurring after primary infection are investigated, considering short, medium and long immunity periods, combined with different values of the disease enhancement factor on secondary infections.

Differently from the simple SIR model that only exhibits a supercritical transcritical bifurcation (in epidemiology the so called forward bifurcation), the simple SIR–SIR type model proposed here exhibits a rich dynamical behavior, with different bifurcations structures leading to solutions that converges to DFE, or to the unique positive endemic equilibria, or to the stable limit cycles due to the occurrence of Hopf bifurcation and Global homoclinic bifurcation. Also, backward bifurcation was showed, displaying a bi-stability in a small parameter region. In addition, several bifurcation structures are identified, including Bogdanov–Takens, cusp and Bautin bifurcations described for the first time in simple models that incorporated intrinsic features of dengue epidemiology.

In detail, for a short immunity period ($\alpha = 52$), the Hopf bifurcation occurs after transcritical bifurcation, changing stability of the endemic equilibria, from stable to unstable. Higher values of enhancement factor lead to unstable endemic equilibria, with solutions converging to a stable limit cycle generated by Hopf bifurcation. Backward bifurcation occurs if, and only if, $\phi > \phi_c > 1$.

For an intermediate temporary immunity period ($\alpha = 2$), backward bifurcation occurs if, and only if, $\phi > \phi_c > 1$. The Hopf bifurcation curve appears after transcritical bifurcation, however, in this scenario, the endemic equilibrium becomes stable after H point.

For a longer temporary immunity period, bi-stability is observed, with the Hopf bifurcation occurring before transcritical bifurcation. Here, the endemic equilibria that exists also for smaller values of $\mathcal{R}_0$ change from unstable to stable in a small set of parameters values where the reproduction number is below 1. Here, long temporary immunity period challenges the control of disease transmission, since even for a subcritical regime of $\mathcal{R}_0 < 1$, the disease would persist. Real life epidemiological scenario related to the mathematical feature of backward bifurcation has been recently described for tuberculosis reinfection dynamics, see e.g. Refs. [38–40].

Tangent (saddle–node), Hopf, and global homoclinic bifurcations were identified, and its occurrence are dependent on the force of infection and immunity period. Tangent bifurcation curves are observed for enhancement factors greater than $\phi_c > 1$. Hopf bifurcation occurs before or after $\mathcal{R}_0 = 1$, depending exclusively on the temporary immunity period. However, by fixing the immunity period, the critical bifurcation point will depend on the enhancement factor value. The global homoclinic bifurcation is always found close to the transcritical

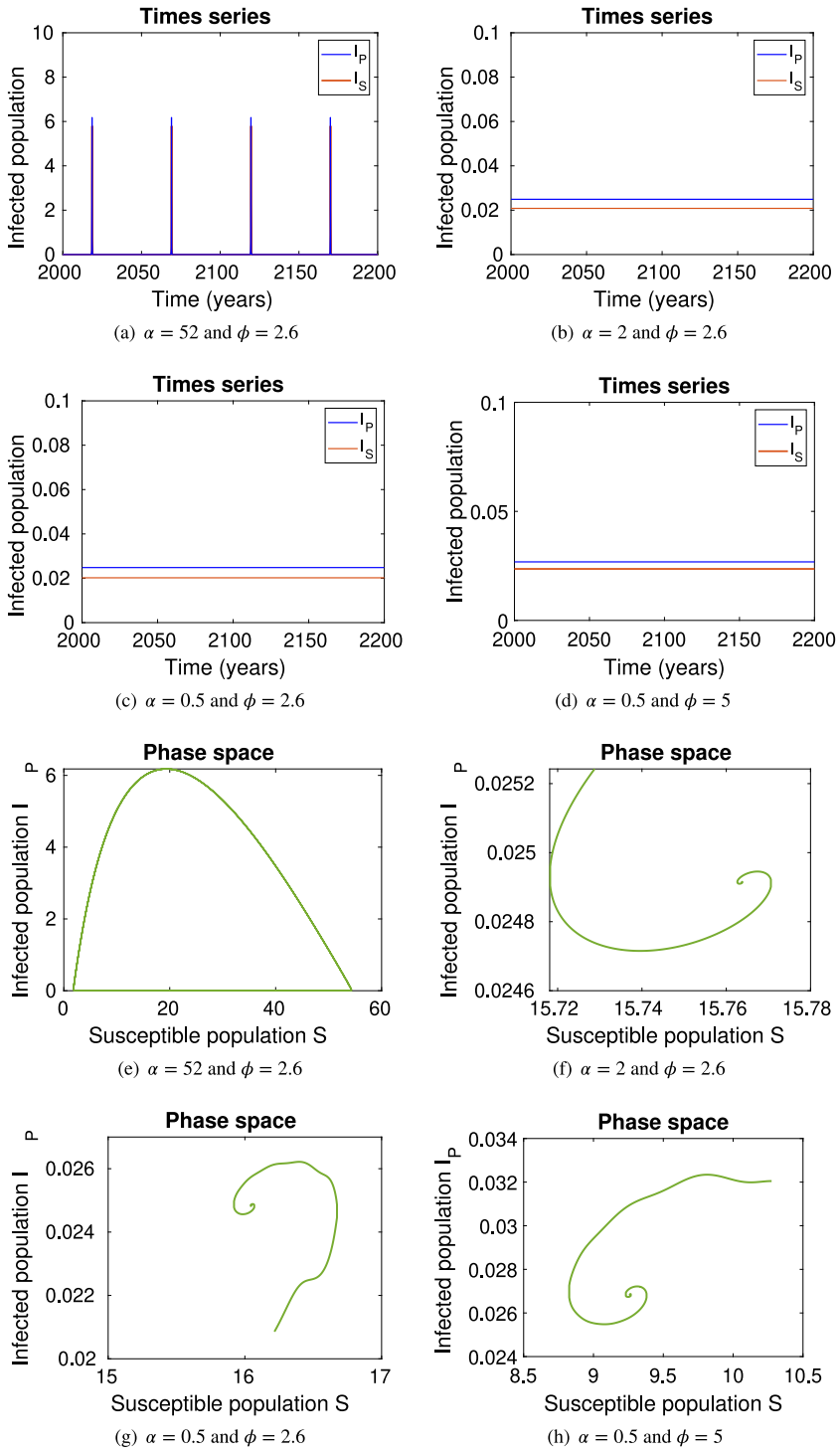

(a) $\alpha = 52$ and $\phi = 2.6$ (b) $\alpha = 2$ and $\phi = 2.6$

(c) $\alpha = 0.5$ and $\phi = 2.6$ (d) $\alpha = 0.5$ and $\phi = 5$

(e) $\alpha = 52$ and $\phi = 2.6$ (f) $\alpha = 2$ and $\phi = 2.6$

(g) $\alpha = 0.5$ and $\phi = 2.6$ (h) $\alpha = 0.5$ and $\phi = 5$

Fig. 9. Times series and phase space plots for the non seasonal SIR–SIR model. With fixed $\beta = 104 = 2\gamma$, the dynamics for different values of temporary immunity α are shown. In (a) and (e), short immunity period ($\alpha = 52$), in (b) and (f), intermediate immunity period ($\alpha = 2$), and in (c), (d), (g) and (h), long immune period ($\alpha = 0.5$). 2000 years of transient are discarded, and the initial conditions are $I_{t_o} = [S_0, I_{P_0}, R_{P_0}, S_{P_0}, I_{S_0}, R_0] = [45.7, 1.63, 0.01, 24.07, 0.08, 28.51]$.

curve, for small values of force of infection, having periodic solutions with very long period lengths and eventually leading to extinction of the disease.

In this minimalist system, chaotic dynamics is only identified after the inclusion of seasonal forcing. However, the combination of temporary immunity and disease enhancement factor play an important role on the model dynamics. We note that without external forcing (non-seasonal), chaotic dynamics can only be found when model formulation considers strain structure of pathogens [3], even though the detailed number of strains, two, three or four, are not the main driving of the system complexity in a multi-strain framework, see Refs. [34,35], which are necessary to describe dengue epidemiological dynamics [14, 15]. Nevertheless, results presented here can be used as additional information for a more extended modeling development, given insights on epidemiological scenarios characterized by chaotic dynamics, in synergy with public health authorities for disease control measures.

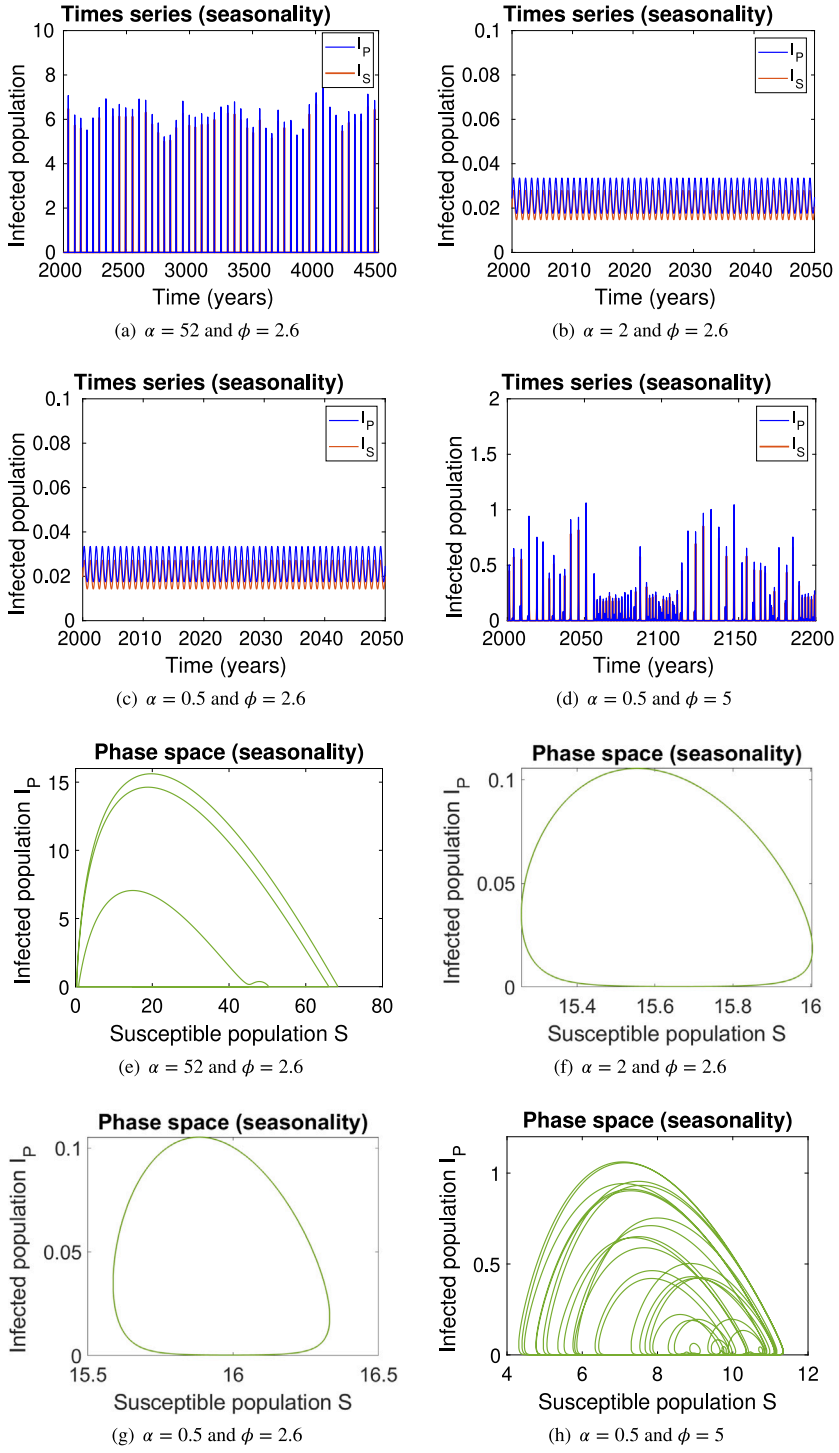

(a) $\alpha = 52$ and $\phi = 2.6$

(b) $\alpha = 2$ and $\phi = 2.6$

(c) $\alpha = 0.5$ and $\phi = 2.6$

(d) $\alpha = 0.5$ and $\phi = 5$

(e) $\alpha = 52$ and $\phi = 2.6$

(f) $\alpha = 2$ and $\phi = 2.6$

(g) $\alpha = 0.5$ and $\phi = 2.6$

(h) $\alpha = 0.5$ and $\phi = 5$

Fig. 10. Times series and phase space plots for the seasonal (non-autonomous) SIR–SIR model. With fixed $\beta = \beta_0 = 104 = 2\gamma$, the dynamics for different values of temporary immunity α are shown. In (a) and (e), short immunity period ($\alpha = 52$), in (b) and (f), intermediate immunity period ($\alpha = 2$), and in (c), (d), (g) and (h), long immune period ($\alpha = 0.5$). 2000 years of transient are discarded, and the initial conditions are $I_{t_o} = [S_0, I_{P_0}, R_{P_0}, S_{P_0}, I_{S_0}, R_0] = [45.7, 1.63, 0.01, 24.07, 0.08, 28.51]$.

Declaration of competing interest

The authors declare the following financial interests/personal relationships which may be considered as potential competing interests: Maira Aguiar reports financial support was provided by Basque Government. Vanessa Steindorf reports financial support was provided by Basque Government. Akhil Srivastav reports financial support was provided by Basque Government. Nico Stollenwerk reports financial support was provided by Basque Government. Maira Aguiar reports financial support was provided by Severo Ochoa Foundation. Vanessa Steindorf reports financial support was provided by Severo Ochoa Foundation. Akhil Srivastav reports financial support was provided by Severo Ochoa Foundation. Nico Stollenwerk reports financial support was provided by Severo Ochoa Foundation. Guest editor of the special issue "New Trends on Mathematical Modelling and Simulation of Biological Systems." - M. Aguiar

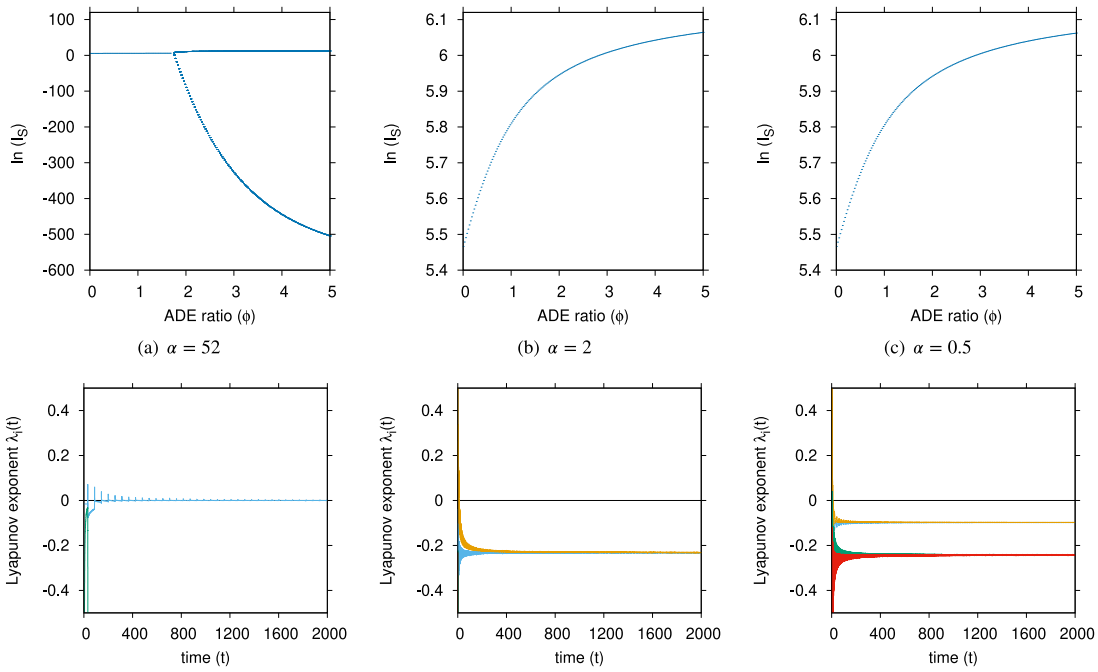

(a) $\alpha = 52$ (b) $\alpha = 2$ (c) $\alpha = 0.5$

(d) $\alpha = 52$ and $\phi = 2.6$ (e) $\alpha = 2$ and $\phi = 2.6$ (f) $\alpha = 0.5$ and $\phi = 2.6$

Fig. 11. For the non seasonal (autonomous) model, bifurcation diagrams, considering the disease enhancement ϕ as a bifurcation parameter, and Lyapunov exponents are shown. For fixed $\phi = 2.6$, and $\beta = \beta_0 = 104 = 2\gamma$, the results for different immunity period α are shown. In (a) and (d) small immunity period ($\alpha = 52$), in (b) and (e) intermediate immunity period ($\alpha = 2$), and in (c) and (f) long immunity period ($\alpha = 0.5$). Note that for non-seasonal scenario, no complex dynamics are observed, and hence, only the Lyapunov exponent for a single parameter value of interest is shown, checking the convergence, which is time dependent, see Refs. [3,36].

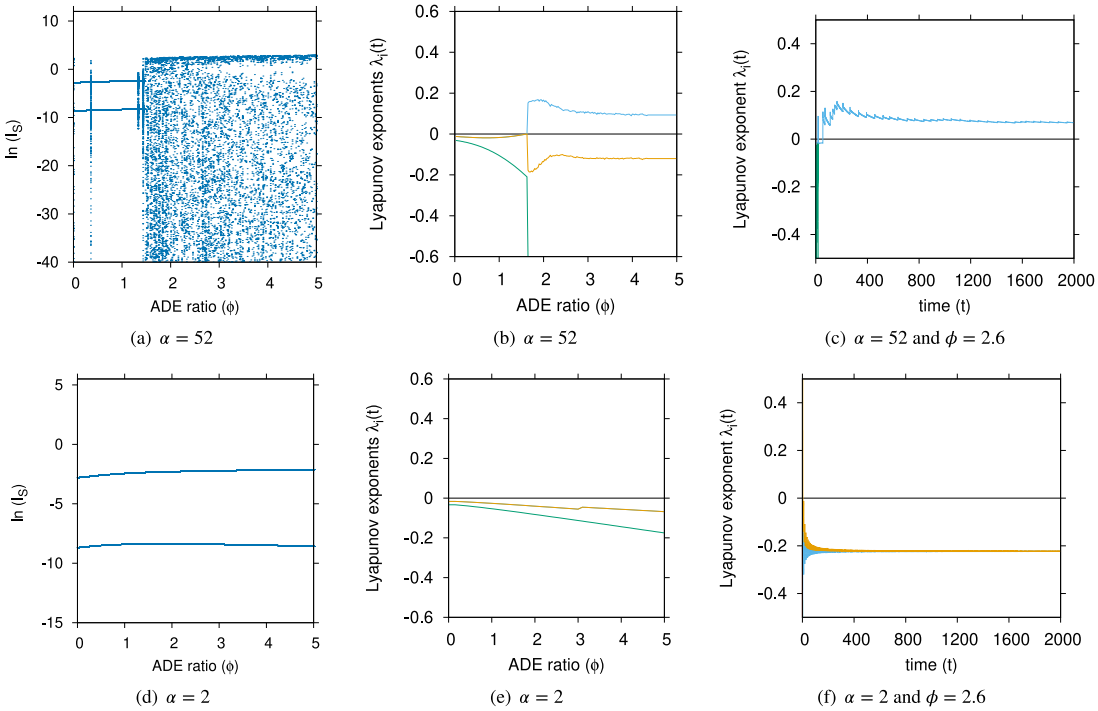

(a) $\alpha = 52$ (b) $\alpha = 52$ (c) $\alpha = 52$ and $\phi = 2.6$

(d) $\alpha = 2$ (e) $\alpha = 2$ (f) $\alpha = 2$ and $\phi = 2.6$

Fig. 12. For the seasonal (non-autonomous) system with short temporary immunity period $\alpha = 52y^{-1}$: in (a) bifurcation diagram, in (b) Lyapunov spectra varying the disease enhancement factor ϕ, and in (c) Lyapunov exponent for $\phi = 2.6$. For the seasonal (non-autonomous) system with an intermediate temporary immunity period $\alpha = 2y^{-1}$: in (a) bifurcation diagram, in (b) Lyapunov spectra varying the disease enhancement factor ϕ, and in (c) Lyapunov exponent for $\phi = 2.6$. the Infection rate is fixed to $\beta = \beta_0 = 104 = 2\gamma$. The other baseline parameter values are shown in Table 1.

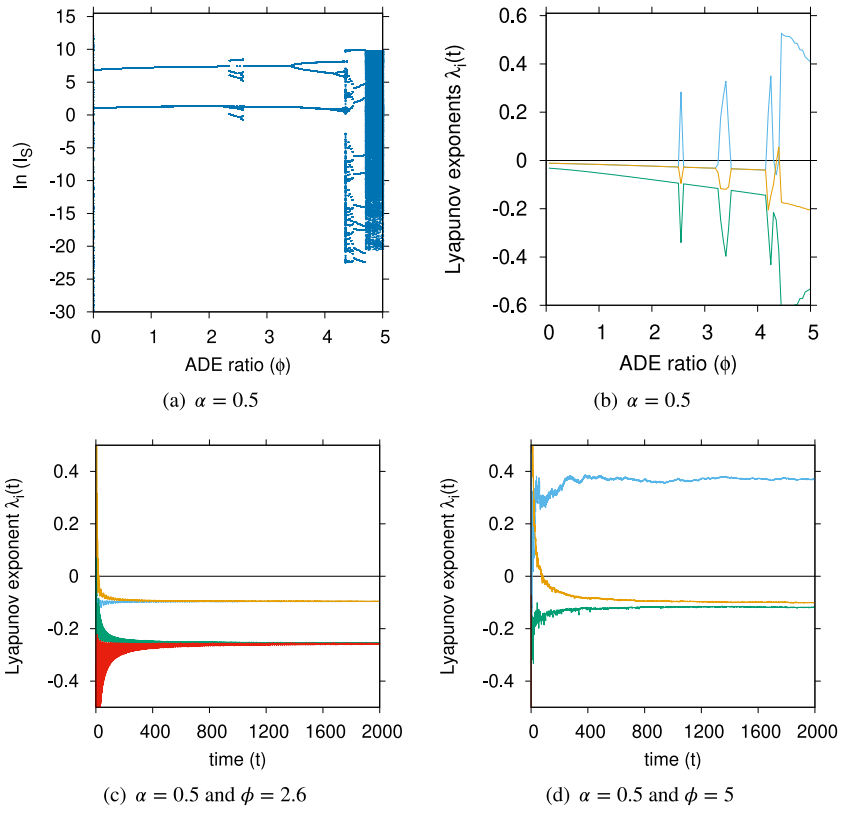

(a) $\alpha = 0.5$ (b) $\alpha = 0.5$

(c) $\alpha = 0.5$ and $\phi = 2.6$ (d) $\alpha = 0.5$ and $\phi = 5$

Fig. 13. For the seasonal (non-autonomous) system, in (a) the bifurcation diagram, considering the disease enhancement ϕ as a bifurcation parameter, for long immunity period α, and in (b), the Lyapunov spectra. Dominant Lyapunov exponents are shown for different enhancement factor values. In (c) $\phi = 2.6$ and in (d) $\phi = 5$. Note that coexisting attractors become visible, e.g., for ϕ values between 2 and 3 (see bifurcation diagram in (a)), hence, depending on the initial conditions, one or another attractor is visited.

Data availability

No data was used for the research described in the article.

Acknowledgments

M.A. has received funding from the European Union's Horizon 2020 research and innovation program under the Marie Skłodowska-Curie grant agreement No 792494. This research is supported by the Basque Government through the BMTF "Mathematical Modeling Applied to Health" Project, BERC 2022-2025 program and by Spanish Ministry of Sciences, Innovation and Universities through BCAM Severo Ochoa accreditation SEV-2017-0718.

Appendix A. Routh–Hurwitz criteria

Theorem 9. *Let $P(\lambda)$ be the polynomial*

$$P(\lambda) = \lambda^n + a_1\lambda^{n-1} + \cdots + a_{n-1}\lambda + a_n,$$

where the coefficients a_i are real, $i = 1, \ldots, n$, define the n Hurwitz Matrix as

$$H_1 = (a_1), H_2 = \begin{pmatrix} a_1 & 1 \\ a_3 & a_2 \end{pmatrix}, H_2 = \begin{pmatrix} a_1 & 1 & 0 \\ a_3 & a_2 & a_1 \\ a_5 & a_4 & a_3 \end{pmatrix}$$

and

$$H_n = \begin{pmatrix} a_1 & 1 & 0 & 0 & \cdots & 0 \\ a_3 & a_2 & a_1 & 1 & \cdots & 0 \\ a_5 & a_4 & a_3 & a_2 & \cdots & 0 \\ \vdots & \vdots & \vdots & \vdots & \cdots & \vdots \\ 0 & 0 & 0 & 0 & \cdots & a_n \end{pmatrix}$$

where $a_j = 0$ if $j > n$. Thus, all the roots of the polynomial $P(\lambda)$ are negative or have negative real part if and only if the determinants of all matrices are positive, that is,

$$\det H_j > 0, \ j = 1, 2, \ldots, n.$$

Appendix B. Long time behavior of solutions for biological set of parameter

For the following time series simulation, the temporary immunity is fixed being 6 months, i.e., $\alpha = 2y^{-1}$, β is varying for values very close to the transcritical bifurcation, that is, β is varying in the way that $\mathcal{R}_0 \approx 1$ and $\phi = 1.5$. Therefore, the time series and phase space plots are explored in order to show the asymptotic behavior of the solutions for parameters values when the backward bifurcation is identified. The initial conditions are different for each plot, and it were chosen using the following method: for each set of parameters, the endemic equilibria was calculated and then perturbing it, by adding $\epsilon = 0.001$ to the value of primary infection and subtracting the same value in the susceptible sub-population (see Figs. 14–19).

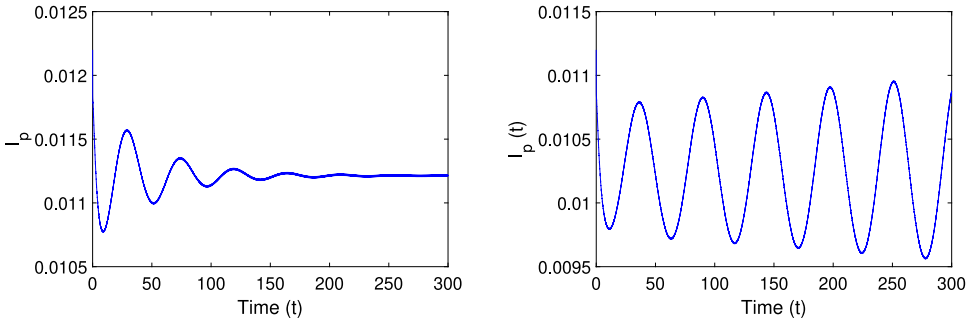

Fig. 14. Time series plots for initial values close to the upper branch state of the backward bifurcation. (a) Solutions approach the fixed point for $\beta = 1.02 * \gamma$. (b) Increasing oscillations for $\beta = 1.01 * \gamma$.

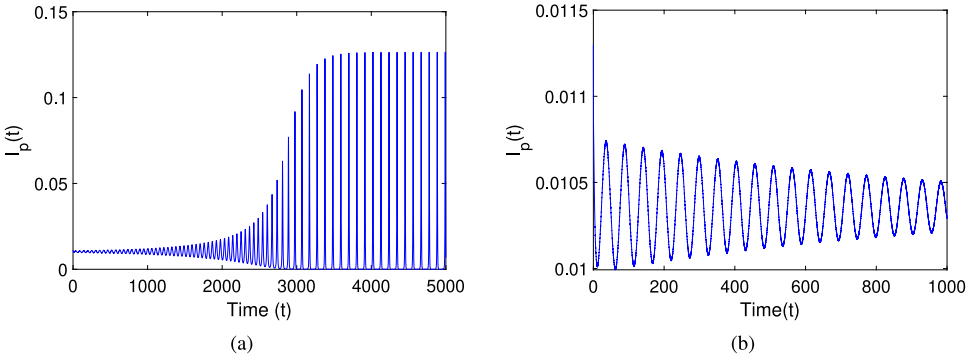

Fig. 15. Time series plots perturbing the upper branch state of the backward bifurcation. (a) Periodic solution for $\beta = 1.010 * \gamma$ (for longer period) showing convergence to a limit cycle. (b) Oscillations decreasing into the fixed point for $\beta = 1.012 * \gamma$.

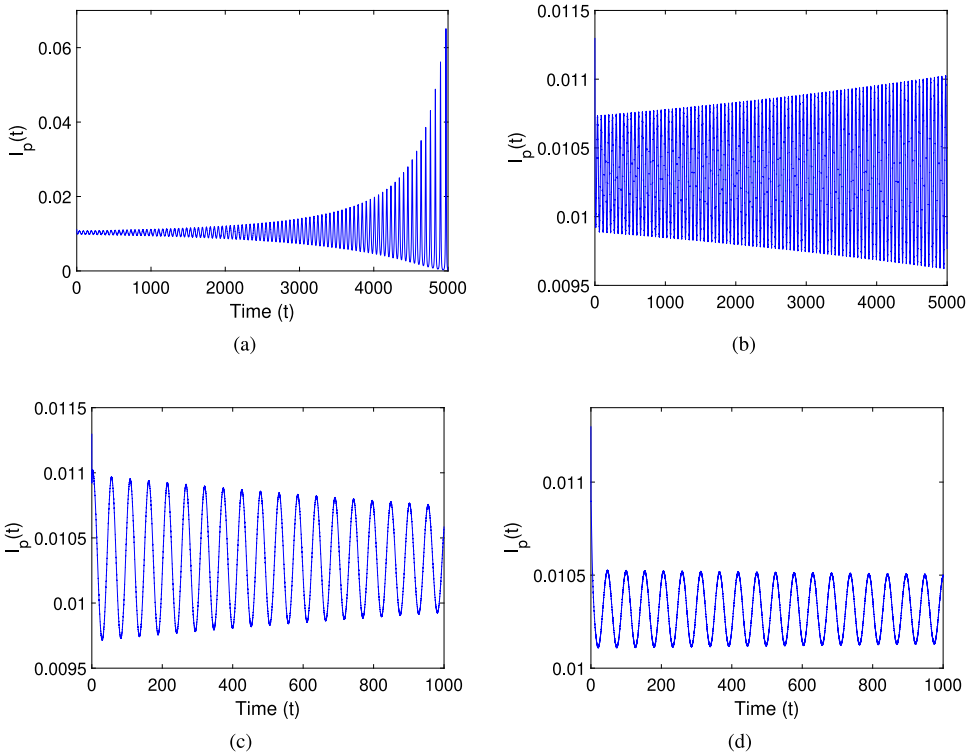

Fig. 16. Time series plots perturbing the upper branch state of the backward bifurcation. (a) Increasing oscillations for $\beta = 1.0105 * \gamma$. (b) Increasing oscillation for $\beta = 1.0110 * \gamma$ (for longer period). (c) Decreasing oscillation into the fixed point for $\beta = 1.0115 * \gamma$. (d) Periodic solutions for $\beta = 1.0112 * \gamma$.

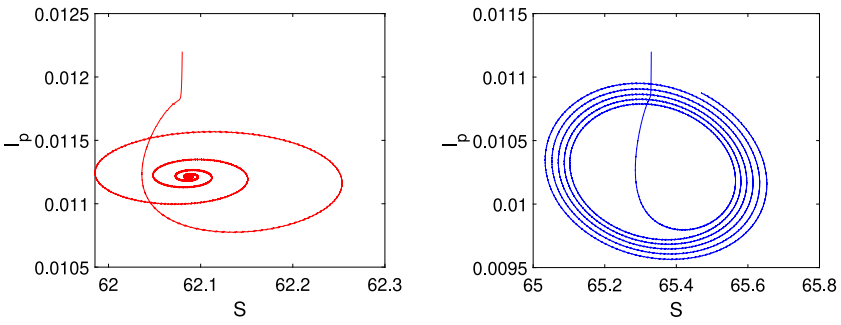

(a) (b)

Fig. 17. Phase space plot (a) to the fixed point for $\beta = 1.02 * \gamma$ (b) to the limit cycle $\beta = 1.01 * \gamma$.

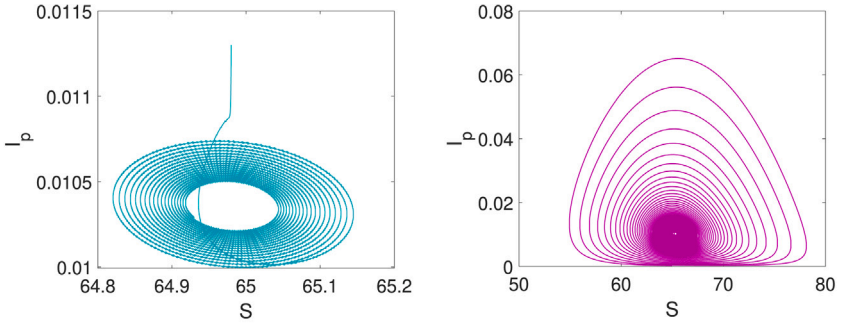

(a) (b)

Fig. 18. Phase space Plot (a) to the fixed point for $\beta = 1.1012 * \gamma$ (b) to a fixed point $\beta = 1.10105 * \gamma$.

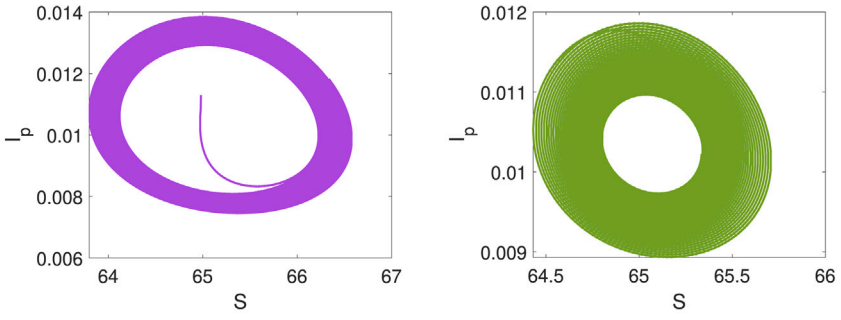

(a) (b)

Fig. 19. Phase space Plot (a) to the limit cycle $\beta = 1.0110 * \gamma$ (b) to the limit cycle $\beta = 1.0115 * \gamma$.

References

[1] Stone L, Olinky R, Huppert A. Seasonal dynamics of recurrent epidemics. Nature 2007;(446):533–6.

[2] Massad E, Stefen M, Mark C, Claudio S, Stollenwerk N, Aguiar M. Scale-free network of a dengue epidemic. Appl Math Comput 2008;195:376–81.

[3] Aguiar M, B.W. Kooi, Stollenwerk N. Epidemiology of dengue fever: A model with temporary cross-immunity and possible secondary infection shows bifurcations and chaotic behaviour in wide parameter regions. Math Model Nat Phenom 2008;3(4):48–70.

[4] Aguiar M, Stollenwerk N, Kooi BW. Torus bifurcations, isolas and chaotic attractors in a simple dengue fever model with ADE and temporary cross immunity. Int J Comput Math 2009;86(10–11):1867–77.

[5] Bhatt S, Gething P, Brady O, et al. The global distribution and burden of dengue. Nature 2013;496:504–7.

[6] Halstead SB. Neutralization and antibody-dependent enhancement of dengue viruses. In: Advances in virus research, vol. 60, Academic Press; 2003, p. 421–67.

[7] Guzman MG, Halstead SB, Artsob H, Buchy P, Farrar J, Gubler DJ, et al. Dengue: a continuing global threat. Nat Rev Microbiol 2010;8(12):S7–16..

[8] Dejnirattisai W, Jumnainsong A, Onsirisakul N, Fitton P, Vasanawathana F, Limpitikul W, et al. Cross-reacting antibodies enhance dengue virus infection in humans. Science 2010;328(5979):745–8.

[9] Katzelnick LC, Gresh L, Halloran EM, Mercado JC, Kuan G, Gordon A, et al. Antibody-dependent enhancement of severe dengue disease in humans. Science 2017;358(6365):929–32.

[10] Fischer DB, Halstead SB. F observations related to pathogenesis of dengue hemorrhagic fever. V. examination of agspecific sequential infection rates using a mathematical model. Yale J Biol Med 1970;42(5):329–49.

[11] Aguiar M, Anam V, Konstantin BB, et al. Mathematical models for dengue fever epidemiology: A 10-year systematic review. Phys Life Rev 2022;40:65–92.

[12] Sebayang AA, Fahlena H, Anam V, Knopoff D, Stollenwerk N, Aguiar M, et al. Modeling dengue immune responses mediated by antibodies: A qualitative study. Biology 2021;10(9).

[13] Anam V, Sebayang AA, Fahlena H, Knopoff D, Stollenwerk N, Soewono E, et al. Modeling dengue immune responses mediated by antibodies: Insights on the biological parameters to describe dengue infections. Comput Math Methods 2022;2022:1–11.

[14] Aguiar M, Ballesteros S, Kooi BW, Stollenwerk N. The role of seasonality and import in a minimalistic multi-strain dengue model capturing differences between primary and secondary infections: Complex dynamics and its implications for data analysis. J Theoret Biol 2011;289:181–96.

[15] Aguiar M, Kooi BW, Martins J, Stollenwerk N. Scaling of stochasticity in dengue hemorrhagic fever epidemics. Math Model Nat Phenom 2012;7(3):1–11.

[16] Ferguson N, Anderson R, Gupta S. The effect of antibody-dependent enhancement on the transmission dynamics and persistence of multiple-strain pathogens. Proc Natl Acad Sci 1999;96(2):790–4.
[17] Wearing HJ, Rohani P. Ecological and immunological determinants of dengue epidemics. Proc Natl Acad Sci 2006;103(31):11802–7.
[18] Kooi BW, Aguiar M, Stollenwerk N. Bifurcation analysis of a family of multi-strain epidemiology models. J Comput Appl Math 2013;252:148–58, Selected papers on Computational and Mathematical Methods in Science and Engineering (CMMSE).
[19] Martcheva M. An introduction to mathematical epidemiology. Texts in applied mathematics, vol. 1, Springer New York, NY; 2015.
[20] Diekmann O, Heesterbeek JAP, Metz JAJ. On the definition and the computation of the basic reproduction ratio R0 in models for infectious diseases in heterogeneous populations. J Math Biol 1990;28(1):365–82.
[21] van den Driessche P, Watmough J. Reproduction numbers and sub-threshold endemic equilibria for compartmental models of disease transmission. Math Biosci 2002;180(1):29–48.
[22] Diekmann O, Heesterbeek J. Mathematical epidemiology of infectious diseases: model building, analysis, and interpretation. Wiley, Hoboken; 2000.
[23] Aguiar M, Van-Dierdonck JB, Stollenwerk N. Reproduction ratio and growth rates: Measures for an unfolding pandemic. PLoS One 2020;15(7):1–14.
[24] Castillo-Chavez C, Song B. Dynamical models of tuberculosis and their applications. Math Biosci Eng 2004;1(2):361–404, 12.
[25] Doedel EJ, Fairgrieve TF, Sandstede B, Champneys AR, Kuznetsov YA, Wang X. AUTO-07P: Continuation and bifurcation software for ordinary differential equations. Technical report, 2007.
[26] Roussel MR. Bifurcation analysis with AUTO. In: Nonlinear dynamics. Morgan & Claypool Publishers; 2019, p. 2053–571, 5–1 to 5–13.
[27] Dhooge A, Govaerts W, Kuznetsov Yu A. MATCONT: A MATLAB package for numerical bifurcation analysis of ODEs. ACM Trans Math Software 2003;29(2):141–64.
[28] MATLAB. Version 7.10.0 (R2010a). Natick, Massachusetts: The MathWorks Inc. 2010.
[29] Wolfram Research, Inc. Mathematica, version 13.0.0. 2021, Champaign, IL.
[30] Lourenço J, Recker M. Viral and epidemiological determinants of the invasion dynamics of novel dengue genotypes. PLoS Negl Trop Dis 2010;4(11):e894.
[31] Reich NG, Shrestha S, King AA, Rohani P, et al. Interactions between serotypes of dengue highlight epidemiological impact of cross-immunity. J R Soc Interface 2013;10.
[32] Steindorf V, Oliva S, Wu J. Cross immunity protection and antibody-dependent enhancement in a distributed delay dynamic model. Math Biosci Eng 2022;19(3):2950–84.
[33] Steindorf V, Oliva S, Wu J, Aguiar M. Effect of general cross-immunity protection and antibody-dependent enhancement in dengue dynamics. Comput Math Methods 2022;2022:22.
[34] Aguiar M, Kooi BW, Rocha F, Ghaffari P, Stollenwerk N. How much complexity is needed to describe the fluctuations observed in dengue hemorrhagic fever incidence data? Ecol Complex 2013;16:31–40, Modelling ecological processes: proceedings of MATE 2011.
[35] Aguiar M, Stollenwerk N, Halstead SB. The impact of the newly licensed dengue vaccine in endemic countries. PLOS Negl Trop Dis 2016;10(12):1–23.
[36] Stollenwerk N, Sommer PF, Kooi B, Mateus L, Ghaffari P, Aguiar M. Hopf and torus bifurcations, torus destruction and chaos in population biology. Ecol Complex 2017;30:91–9, Dynamical Systems In Biomathematics.
[37] Grygiel Krzysztof, Szlachetka P. Lyapunov exponents analysis of autonomous and nonautonomous sets of ordinary differential equations. Acta Phys Polon B 1995;26.
[38] Wangari IM, Stone L. Backward bifurcation and hysteresis in models of recurrent tuberculosis. PLoS One 2018;13:e0194256.
[39] Caminero JA, Pena MJ, Campos-Herrero MI, et al. Exogenous reinfection with tuberculosis on a European island with a moderate incidence of disease. Am J Respir Crit Care Med 2001;163:717–20.
[40] Cohen T, Murray M. Incident tuberculosis among recent US immigrants and exogenous reinfection. Emerg Infect Dis 2005;11:725–8.